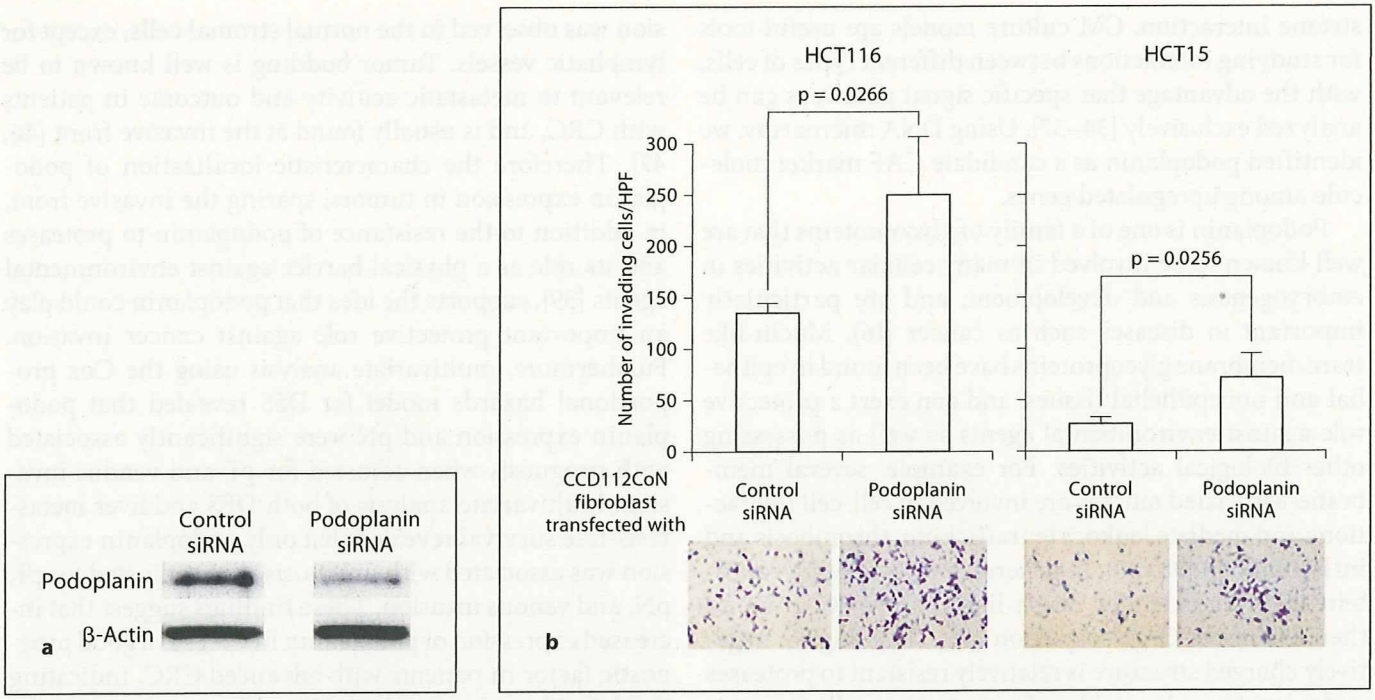

Fig. 3. Podoplanin expression in CCD112CoN fibroblast cells transfected with siRNAs and invasiveness of the cocultured CRC cell lines HCT116 and HCT15. **a** Western blotting using anti-D2–40 antibody (1:100; Dako) in the CCD112CoN fibroblast cells transfected with siRNAs. Podoplanin siRNA reduced podoplanin expression at the protein level almost completely. β-Actin was used as a loading control. **b** Invasiveness of HCT116 and HCT15 cells cocultured with fibroblasts transfected with podoplanin siRNA and control siRNA and in the Matrigel invasion system. After 24 h of coculture, CRC cell lines cocultured with fibroblasts transfected with podoplanin siRNA exhibited a 1.8- to 2.6-fold increase in the number of cells invading the Matrigel-coated insert. HPF = High-power field.

Table 3. Multivariate Cox proportional hazards analysis in patients with advanced CRC (stages II and III)

Prognostic factors	Disease-specific survival			Recurrence-free survival			Liver metastasis-free survival		
	HR	95% CI	p value	HR	95% CI	p value	HR	95% CI	p value
Expression of podoplanin (group A/group B)	0.161	0.037–0.708	0.0157	0.153	0.046–0.510	0.0023	0.089	0.012–0.682	0.0198
Depth of invasion (T2, T3/T4)	0.339	0.075–1.523	0.1582	0.308	0.089–1.066	0.0630	0.396	0.089–1.775	0.2264
Lymph node metastasis (absence/presence)	0.237	0.066–0.849	0.0270	0.488	0.201–1.184	0.1125	0.864	0.297–2.515	0.7888
Venous invasion (presence/absence)	0.858	0.269–2.739	0.7956	1.517	0.551–4.175	0.4194	5.745	0.727–45.380	0.0973

HR = Hazard ratio; CI = confidence interval.

planin, the number of invading cells was significantly increased ($p = 0.027$ and $p = 0.026$, Student's t test for coculture with HCT116 and HCT15, respectively; fig. 3b). As a negative control, when fibroblasts transfected with control siRNA and podoplanin siRNA were cultured only in CM-HT29 without CRC cell lines, almost no invading cells were evident (data not shown).

Discussion

To help understand the difference between CAFs and uninvolved fibroblasts, and to further evaluate the role of CAFs, we compared their genome-wide expression profiles using in vitro CM culture models in which soluble factors originating from cancer cells exerted a paracrine action on the surrounding fibroblasts involved in tumor-

stroma interaction. CM culture models are useful tools for studying interactions between different types of cells, with the advantage that specific signal pathways can be analyzed exclusively [34–37]. Using DNA microarray, we identified podoplanin as a candidate CAF marker molecule among upregulated genes.

Podoplanin is one of a family of glycoproteins that are well known to be involved in many cellular activities in embryogenesis and development, and are particularly important in diseases such as cancer [16]. Mucin-like transmembrane glycoproteins have been found in epithelial and nonepithelial tissues, and can exert a protective role against environmental agents as well as possessing other biological activities. For example, several membrane-associated mucins are involved in cell-cell interactions and mediate leukocyte trafficking, thrombosis and inflammation [38–40]. In general, mucin-type glycoproteins have an extended brush-like conformation due to their extensive O-glycosylation [39]. This highly negatively charged structure is relatively resistant to proteases and provides a physical barrier protecting cells from environmental agents.

In the present study, immunohistochemical localization of podoplanin was confined exclusively to CAFs in the cancer stroma. Normal stroma, epithelial cells and tumor cells were completely negative for podoplanin in all cases tested, and only lymphatic vessels were positive. Podoplanin expression in CAFs of cancer stroma was significantly correlated with more distal tumor localization and a shallower depth of tumor invasion. Invasion of CRC cell lines was augmented upon coculture with fibroblasts in which podoplanin expression was reduced by siRNA. These results indicate that podoplanin could play an important protective role against cancer invasion.

Expression of podoplanin by cancer cells of oral and uterine cervix squamous cell carcinoma has been reported to be associated with prognosis [41, 42]. However, previous studies have found that adenocarcinoma cells rarely express podoplanin [43, 44]. Podoplanin-positive CAFs are reportedly present in invasive adenocarcinoma of the lung, but not in noninvasive adenocarcinoma [45]. Podoplanin expression by CAFs is reported to be significantly associated with a poor outcome in patients with lung adenocarcinoma. However, multivariate analysis failed to show that podoplanin expression was an independent prognostic factor [45]. In the present study, the localization of podoplanin expression was intriguing because it was seen in CAFs located mainly in the superficial to deep area of the tumor, sparing the invasive front where tumor budding is often observed. No podoplanin expression was observed in the normal stromal cells, except for lymphatic vessels. Tumor budding is well known to be relevant to metastatic acitivity and outcome in patients with CRC, and is usually found at the invasive front [46, 47]. Therefore the characteristic localization of podoplanin expression in tumors, sparing the invasive front, in addition to the resistance of podoplanin to proteases and its role as a physical barrier against environmental agents [39], supports the idea that podoplanin could play an important protective role against cancer invasion. Furthermore, multivariate analysis using the Cox proportional hazards model for DSS revealed that podoplanin expression and pN were significantly associated with prognosis when adjusted for pT and venous invasion. Multivariate analysis of both DFS and liver metastasis-free survival revealed that only podoplanin expression was associated with prognosis when adjusted for pT, pN, and venous invasion. These findings suggest that increased expression of podoplanin in CAFs is a good prognostic factor in patients with advanced CRC, indicating the defensive role of podoplanin against tumor invasion. In terms of clinical use, podoplanin expression in CRC might be helpful for selecting patients who should undergo adjuvant chemotherapy, or those for whom it is unnecessary. However, in order for podoplanin expression to be applied for practical clinical care, it must be validated in a large-scale prospective clinical trial.

Furthermore, our coculture invasion assay indicated that podoplanin expressed in CAFs could have a suppressive effect on the invasion of tumor cells, although it is not yet clear whether CAFs have both an inductive and a suppressive effect on tumor progression and regulate tumorigenesis. Other constituents of the desmoplastic extracellular matrix have also been shown to inhibit tumor progression. For example, injection of L-3, 4-dehydroproline, which inhibits the formation of collagen fibrils, increases tumor cell invasion in mice with B16F10 melanoma subcutaneous tumors [48]. In addition, extracellular matrix accumulation in tumors contributes to increased interstitial fluid pressure and hinders the diffusion of macromolecules and oxygen, leading to tumor cell necrosis [49, 50]. The overall effect of altered extracellular matrix in tumors and the effect of CAFs during tumor progression are still poorly understood. Further studies directed at disrupting the complex interaction between tumor cells and stromal composition may define new strategies for diagnosis of tumors and suitable therapeutic interventions.

In conclusion, podoplanin, a mucin-type transmembrane glycoprotein, was found to be upregulated in CAFs

in vitro and to be overexpressed in CAFs surrounding CRC cells in vivo. Multivariate analysis of both DFS and liver metastasis-free survival revealed that only podoplanin expression was associated with prognosis when adjusted for pT, pN, and venous invasion. In addition, invasiveness of CRC cells was increased significantly by coculture with podoplanin-suppressed CAFs. These findings suggest that increased podoplanin expression in stromal fibroblasts is a significant indicator of good prognosis in patients with advanced CRC, reflecting its defensive role against cancer invasion.

Acknowledgement

This study was supported by a grant-in-aid for the Third Term Comprehensive 10-Year Strategy for Cancer Control from the Ministry of Health, Labor and Welfare of Japan. T. Y. is a recipient of a Research Resident Fellowship from the Foundation for Promotion of Cancer Research in Japan.

References

1 Bhowmick NA, Neilson EG, Moses HL: Stromal fibroblasts in cancer initiation and progression. Nature 2004;432:332–337.
2 De Wever O, Mareel M: Role of tissue stroma in cancer cell invasion. J Pathol 2003;200:429–447.
3 Kalluri R, Zeisberg M: Fibroblasts in cancer. Nat Rev Cancer 2006;6:392–401.
4 Micke P, Ostman A: Exploring the tumour environment: cancer-associated fibroblasts as targets in cancer therapy. Expert Opin Ther Targets 2005;9:1217–1233.
5 Bhowmick NA, Chytil A, Plieth D, et al: TGF-β signaling in fibroblasts modulates the oncogenic potential of adjacent epithelia. Science 2004;303:848–851.
6 Orimo A, Gupta PB, Sgroi DC, et al: Stromal fibroblasts present in invasive human breast carcinomas promote tumor growth and angiogenesis through elevated SDF-1/CXCL12 secretion. Cell 2005;121:335–348.
7 Olumi AF, Grossfeld GD, Hayward SW, Carroll PR, Tlsty TD, Cunha GR: Carcinoma-associated fibroblasts direct tumor progression of initiated human prostatic epithelium. Cancer Res 1999;59:5002–5011.
8 Dimanche-Boitrel MT, Vakaet L Jr, Pujuguet P, et al: In vivo and in vitro invasiveness of a rat colon-cancer cell line maintaining E-cadherin expression: an enhancing role of tumor-associated myofibroblasts. Int J Cancer 1994;56:512–521.
9 Sternlicht MD, Lochter A, Sympson CJ, et al: The stromal proteinase MMP3/stromelysin-1 promotes mammary carcinogenesis. Cell 1999;98:137–146.
10 Lochter A, Galosy S, Muschler J, Freedman N, Werb Z, Bissell MJ: Matrix metalloproteinase stromelysin-1 triggers a cascade of molecular alterations that leads to stable epithelial-to-mesenchymal conversion and a premalignant phenotype in mammary epithelial cells. J Cell Biol 1997;139:1861–1872.
11 Cornil I, Theodorescu D, Man S, Herlyn M, Jambrosic J, Kerbel RS: Fibroblast cell interactions with human melanoma cells affect tumor cell growth as a function of tumor progression. Proc Natl Acad Sci USA 1991;88:6028–6032.
12 Mishima K, Kato Y, Kaneko MK, Nishikawa R, Hirose T, Matsutani M: Increased expression of podoplanin in malignant astrocytic tumors as a novel molecular marker of malignant progression. Acta Neuropathol (Berl) 2006;111:483–488.
13 Yuan P, Temam S, El-Naggar A, et al: Overexpression of podoplanin in oral cancer and its association with poor clinical outcome. Cancer 2006;107:563–569.
14 Schacht V, Dadras SS, Johnson LA, Jackson DG, Hong YK, Detmar M: Up-regulation of the lymphatic marker podoplanin, a mucin-type transmembrane glycoprotein, in human squamous cell carcinomas and germ cell tumors. Am J Pathol 2005;166:913–921.
15 Zimmer G, Oeffner F, Von Messling V, et al: Cloning and characterization of gp36, a human mucin-type glycoprotein preferentially expressed in vascular endothelium. Biochem J 1999;341:277–284.
16 Brockhausen I, Schutzbach J, Kuhns W: Glycoproteins and their relationship to human disease. Acta Anat (Basel) 1998;161:36–78.
17 Martin-Villar E, Scholl FG, Gamallo C, et al: Characterization of human PA2.26 antigen (T1α-2, podoplanin), a small membrane mucin induced in oral squamous cell carcinomas. Int J Cancer 2005;113:899–910.
18 Ordonez NG: Podoplanin: a novel diagnostic immunohistochemical marker. Adv Anat Pathol 2006;13:83–88.
19 Breiteneder-Geleff S, Soleiman A, Kowalski H, et al: Angiosarcomas express mixed endothelial phenotypes of blood and lymphatic capillaries: podoplanin as a specific marker for lymphatic endothelium. Am J Pathol 1999;154:385–394.
20 Schacht V, Ramirez MI, Hong YK, et al: T1α/podoplanin deficiency disrupts normal lymphatic vasculature formation and causes lymphedema. Embo J 2003;22:3546–3556.
21 Wicki A, Lehembre F, Wick N, Hantusch B, Kerjaschki D, Christofori G: Tumor invasion in the absence of epithelial-mesenchymal transition: podoplanin-mediated remodeling of the actin cytoskeleton. Cancer Cell 2006;9:261–272.
22 Sugimoto Y, Watanabe M, Oh-hara T, Sato S, Isoe T, Tsuruo T: Suppression of experimental lung colonization of a metastatic variant of murine colon adenocarcinoma 26 by a monoclonal antibody 8F11 inhibiting tumor cell-induced platelet aggregation. Cancer Res 1991;51:921–925.
23 Watanabe M, Okochi E, Sugimoto Y, Tsuruo T: Identification of a platelet-aggregating factor of murine colon adenocarcinoma as determined by monoclonal antibodies. Cancer Res 1988;48:6411–6416.
24 Kato Y, Kaneko M, Sata M, Fujita N, Tsuruo T, Osawa M: Enhanced expression of Aggrus (T1α/podoplanin), a platelet-aggregation-inducing factor in lung squamous cell carcinoma. Tumour Biol 2005;26:195–200.
25 Kimura N, Kimura I: Podoplanin as a marker for mesothelioma. Pathol Int 2005;55:83–86.
26 Ordonez NG: D2–40 and podoplanin are highly specific and sensitive immunohistochemical markers of epithelioid malignant mesothelioma. Hum Pathol 2005;36:372–380.
27 Roy S, Chu A, Trojanowski JQ, Zhang PJ: D2–40, a novel monoclonal antibody against the M2A antigen as a marker to distinguish hemangioblastomas from renal cell carcinomas. Acta Neuropathol (Berl) 2005;109:497–502.

28 Kato Y, Sasagawa I, Kaneko M, Osawa M, Fujita N, Tsuruo T: Aggrus: a diagnostic marker that distinguishes seminoma from embryonal carcinoma in testicular germ cell tumors. Oncogene 2004;23:8552–8556.
29 Shibahara J, Kashima T, Kikuchi Y, Kunita A, Fukayama M: Podoplanin is expressed in subsets of tumors of the central nervous system. Virchows Arch 2006;448:493–499.
30 Mishima K, Kato Y, Kaneko MK, et al: Podoplanin expression in primary central nervous system germ cell tumors: a useful histological marker for the diagnosis of germinoma. Acta Neuropathol (Berl) 2006;111:563–568.
31 Gandarillas A, Scholl FG, Benito N, Gamallo C, Quintanilla M: Induction of PA2.26, a cell-surface antigen expressed by active fibroblasts, in mouse epidermal keratinocytes during carcinogenesis. Mol Carcinog 1997;20:10–18.
32 Sobin LH, Fleming ID: TNM Classification of Malignant Tumors, ed 5 (1997). Union Internationale contre le Cancer and the American Joint Committee on Cancer. Cancer 1997;80:1803–1804.
33 World Health Organization: Classification of Tumours. Lyon, IARC Press, 2000.
34 DeCosse JJ, Gossens C, Kuzma JF, Unsworth BR: Embryonic inductive tissues that cause histologic differentiation of murine mammary carcinoma in vitro. J Natl Cancer Inst 1975;54:913–922.
35 DeCosse JJ, Gossens CL, Kuzma JF, Unsworth BR: Breast cancer: induction of differentiation by embryonic tissue. Science 1973;181:1057–1058.
36 Cooper M, Pinkus H: Intrauterine transplantation of rat basal cell carcinoma as a model for reconversion of malignant to benign growth. Cancer Res 1977;37:2544–2552.
37 Maehara N, Matsumoto K, Kuba K, Mizumoto K, Tanaka M, Nakamura T: NK4, a four-kringle antagonist of HGF, inhibits spreading and invasion of human pancreatic cancer cells. Br J Cancer 2001;84:864–873.
38 Gendler SJ, Spicer AP: Epithelial mucin genes. Annu Rev Physiol 1995;57:607–634.
39 Hilkens J, Ligtenberg MJ, Vos HL, Litvinov SV: Cell membrane-associated mucins and their adhesion-modulating property. Trends Biochem Sci 1992;17:359–363.
40 Varki A: Selectin ligands. Proc Natl Acad Sci USA 1994;91:7390–7397.
41 Yuan P, Temam S, El-Naggar A, Zhou X, Liu DD, Lee JJ, Mao L: Overexpression of podoplanin in oral cancer and its association with poor clinical outcome. Cancer 2006;107:563–569.
42 Dumoff KL, Chu CS, Harris EE, Holtz D, Xu X, Zhang PJ, ACS G: Low podoplanin expression in pretreatment biopsy material predicts poor prognosis in advanced-stage squamous cell carcinoma of the uterine cervix treated by primary radiation. Mod Pathol 2006;19:708–716.
43 Ordonez NG: D2-40 and podoplanin are highly specific and sensitive immunohistochemical markers of epithelioid malignant mesothelioma. Hum Pathol 2005;36:372–380.
44 Chu AY, Litzky LA, Pasha TL, Acs G, Zhang PJ: Utility of D2-40, a novel mesothelial marker, in the diagnosis of malignant mesothelioma. Mod Pathol 2005;18:105–110.
45 Kawase A, Ishii G, Nagai K, Ito T, Nagano T, Murata Y, Hishida T, Nishimura M, Yoshida J, Suzuki K, Ochiai A: Podoplanin expression by cancer associated fibroblasts predicts poor prognosis of lung adenocarcinoma. Int J Cancer 2008;123:1053–1059.
46 Okuyama T, Oya M, Ishikawa H: Budding as a risk factor for lymph node metastasis in pT1 or pT2 well-differentiated colorectal adenocarcinoma. Dis Colon Rectum 2002;45:628–634.
47 Ueno H, Price AB, Wilkinson KH, Jass JR, Mochizuki H, Talbot IC: A new prognostic staging system for rectal cancer. Ann Surg 2004;240:832–839.
48 Barsky SH, Gopalakrishna R: Increased invasion and spontaneous metastasis of BL6 melanoma with inhibition of the desmoplastic response in C57 BL/6 mice. Cancer Res 1987;47:1663–1667.
49 Netti PA, Berk DA, Swartz MA, Grodzinsky AJ, Jain RK: Role of extracellular matrix assembly in interstitial transport in solid tumors. Cancer Res 2000;60:2497–2503.
50 Brown EB, Boucher Y, Nasser S, Jain RK: Measurement of macromolecular diffusion coefficients in human tumors. Microvasc Res 2004;67:231–236.

Oncogene (2009) 28, 2738–2744

www.nature.com/onc

ORIGINAL ARTICLE

Chromatin remodeling at Alu repeats by epigenetic treatment activates silenced *microRNA-512-5p* with downregulation of *Mcl-1* in human gastric cancer cells

Y Saito[1], H Suzuki[1], H Tsugawa[1], I Nakagawa[1], J Matsuzaki[1], Y Kanai[2] and T Hibi[1]

[1]*Division of Gastroenterology and Hepatology, Department of Internal Medicine, Keio University School of Medicine, Shinjuku-ku, Tokyo, Japan and* [2]*Pathology Division, National Cancer Center Research Institute, Chuo-ku, Tokyo, Japan*

Epigenetic therapy using DNA methylation inhibitors and histone deacetylase (HDAC) inhibitors has clinical promise for the treatment of human malignancies. To investigate roles of microRNAs (miRNAs) on epigenetic therapy of gastric cancer, the miRNA expression profile was analysed in human gastric cancer cells treated with 5-aza-2′-deoxycytidine (5-Aza-CdR) and 4-phenylbutyric acid (PBA). miRNA microarray analysis shows that most of miRNAs activated by 5-Aza-CdR and PBA in gastric cancer cells are located at Alu repeats on chromosome 19. Analyses of chromatin modification show that DNA demethylation and HDAC inhibition at Alu repeats activates silenced *miR-512-5p* by RNA polymerase II. In addition, activation of *miR-512-5p* by epigenetic treatment induces suppression of *Mcl-1*, resulting in apoptosis of gastric cancer cells. These results suggest that chromatin remodeling at Alu repeats plays critical roles in the regulation of miRNA expression and that epigenetic activation of silenced Alu-associated miRNAs could be a novel therapeutic approach for gastric cancer.
Oncogene (2009) **28**, 2738–2744; doi:10.1038/onc.2009.140; published online 8 June 2009

Keywords: miRNA; DNA methylation; histone modification; epigenetic treatment; Alu repeats; gastric cancer

Introduction

Chromatin-modifying drugs such as DNA methylation inhibitors and histone deacetylase (HDAC) inhibitors are emerging as effective agents for 'epigenetic therapy' of cancer (Yoo and Jones, 2006; Gal-Yam *et al.*, 2008). In fact, the DNA methylation inhibitors 5-aza-2′-deoxycytidine (5-Aza-CdR) and 5-azacytidine (5-Aza-CR) were recently approved by the Food and Drug Administration for the treatment of myelodysplastic syndrome, and many HDAC inhibitors such as 4-phenylbutyric acid (PBA) are under clinical trials (Yoo and Jones, 2006). However, the molecular mechanisms underlying anticancer effect of these drugs are not fully understood.

MicroRNAs (miRNAs) are small non-coding RNAs, which can downregulate various target genes. miRNAs are expressed in a tissue-specific manner and have important functions in cellular proliferation, apoptosis and differentiation. Recent studies have indicated that aberrant expression of miRNAs contributes to the initiation and progression of human malignancies (Calin and Croce, 2006a, b). We have recently shown that some miRNAs are located near CpG islands and that expression of these miRNAs is regulated by alterations in DNA methylation and histone modification on their CpG islands (Saito and Jones, 2006; Saito *et al.*, 2006).

As the stomach is an organ in which epigenetic alterations due to *Helicobacter pylori* infection or various exogenous antigen exposures are frequently observed (Esteller, 2002), we are prompted to investigate miRNA expression profile in gastric cancer cells with epigenetic treatment. Interestingly, microarray analysis of AGS gastric cancer cells shows that most of the miRNAs, which are dramatically activated by 5-Aza-CdR and PBA, are located at Alu repeats on chromosome 19. Alu elements are ~280 bp in length and consist of two similar, but distinct, monomers linked by an oligo (dA) tract. It has been reported that Alu repeats in the miRNA cluster on chromosome 19 can function as RNA polymerase III (Pol III) promoters of miRNAs (Borchert *et al.*, 2006). Here we show that chromatin remodeling at Alu repeats by DNA demethylation and HDAC inhibition can activate expression of Alu-associated miRNAs, which can downregulate target oncogenes in human gastric cancer cells.

Results

miRNAs activated by epigenetic treatment in gastric cancer cells are located at Alu repeats on chromosome 19

To identify miRNAs, which are regulated by DNA demethylation and HDAC inhibition, we carried out miRNA microarray analysis. The miRNA expression profile of AGS human gastric cancer cells showed that 115 out of 470 miRNAs were differentially expressed by the treatment with 5-Aza-CdR and PBA ($P<0.01$).

Correspondence: Dr H Suzuki, Division of Gastroenterology and Hepatology, Department of Internal Medicine, Keio University School of Medicine, 35 Shinanomachi, Shinjuku-ku, Tokyo 160-8582, Japan. E-mail: hsuzuki@sc.itc.keio.ac.jp
Received 11 December 2008; revised 23 March 2009; accepted 18 April 2009; published online 8 June 2009

Interestingly, 14 out of top 15 miRNAs (93%) upregulated by epigenetic treatment are located in the miRNA cluster on chromosome 19 (Figure 1a) (Bentwich *et al.*, 2005). These miRNAs are interspersed among Alu repeats which can function as their promoters (Borchert *et al.*, 2006). We have recently reported that epigenetic treatment of T24 bladder cancer cells induced activation of only 5 Alu-associated miRNAs in top 15 miRNAs (33%) (Figure 1a) (Saito *et al.*, 2006). In addition, the signal ratios of Alu-associated miRNAs after epigenetic treatment in AGS cells compared with untreated cells were much higher than those in T24 cells. Therefore, activation of Alu-associated miRNAs by DNA demethylation and HDAC inhibition seems to be more specific in gastric cancer cells compared with bladder cancer cells.

To confirm the miRNA microarray data, we carried out quantitative reverse transcriptase (RT)–PCR analyses for *miR-512-5p, -517b, -526b, -518b* and *-515-5p* in AGS cells treated with 5-Aza-CdR and PBA. As shown in Figure 1b, all miRNAs examined were silenced before treatment and dramatically activated by 5-Aza-CdR and PBA treatment, which is consistent with the microarray data. Other gastric cancer cell lines (TMK1 and MKN45) also showed marked upregulation of *miR-512-5p* and *miR-517b* by epigenetic treatment (Figure 1c).

DNA demethylation and HDAC inhibition at Alu repeats activates silenced miR-512-5p

As epigenetic treatment remarkably upregulate expression of Alu-associated miRNAs, we examined DNA methylation and histone modification at the Alu promoter region of *miR-512* by bisulfite genomic sequencing and chromatin immunoprecipitation (ChIP) assay, respectively (Figures 2a and b). It was found that although the Alu promoter regions of *miR-512* were completely methylated (100%) in untreated AGS cells, DNA methylation levels were reduced to 20% after epigenetic treatment (Figure 2a).

Both acetylated histone H3 and methylated histone H3-lysine 4 (K4) are associated with an open chromatin structure and active gene expression. Significant increases in the levels of both acetylated histone H3 and methylated histone H3-K4 were found at the Alu promoter region of *miR-512* in AGS cells treated with 5-Aza-CdR and PBA (Figure 2b). These findings indicate that dense DNA methylation and closed chromatin structure at Alu repeats are associated with a silent state of *miR-512-5p*, and that chromatin remodeling at Alu repeats by DNA demethylation and HDAC inhibition activate silenced *miR-512-5p*.

a AGS

No.	microRNA	Ratio	Locus	Alu
1	miR-512-5p	136	19q13	■
2	miR-517b	84	19q13	■
3	miR-517a	79	19q13	■
4	miR-526b	42	19q13	■
5	miR-518b	55	19q13	■
6	miR-515-5p	45	19q13	■
7	miR-512-3p	50	19q13	■
8	miR-516-5p	50	19q13	■
9	miR-520h	29	19q13	■
10	miR-524*	26	19q13	■
11	miR-127	23	14q32	
12	miR-520g	23	19q13	■
13	miR-526a	22	19q13	■
14	miR-520a*	21	19q13	■
15	miR-525	20	19q13	■

T24

No.	microRNA	Ratio	Locus	Alu
1	miR-127	49	14q32	
2	miR-377	44	14q32	
3	miR-494	36	14q32	
4	miR-495	31	14q32	
5	miR-517a	27	19q13	■
6	miR-516-5p	26	19q13	■
7	miR-517b	10	19q13	■
8	miR-512-3p	8	19q13	■
9	miR-192	6	11q13	
10	miR-193b	6	16p13	
11	miR-134	4	14q32	
12	miR-182	4	7q32	
13	miR-368	4	14q32	
14	miR-498	4	19q13	■
15	miR-126	3	9q34	

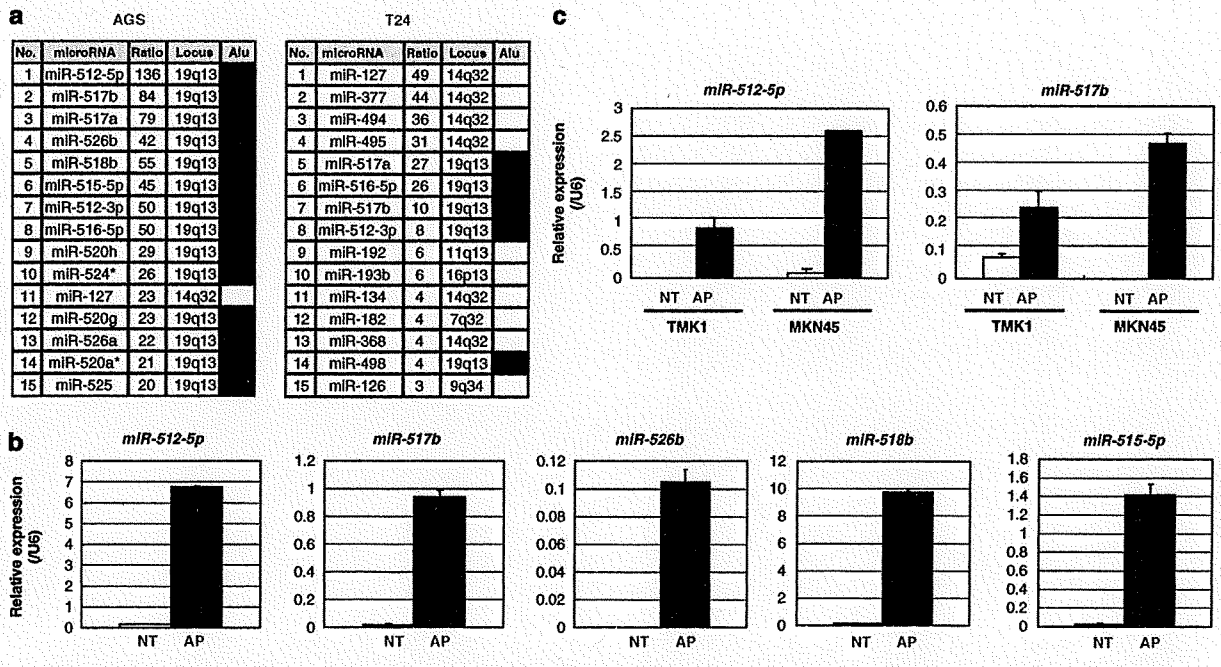

Figure 1 Expression patterns of Alu-associated microRNAs (miRNAs) in human gastric cancer cells treated with 5-aza-2′-deoxycytidine (5-Aza-CdR) and 4-phenylbutyric acid (PBA). (**a**) miRNAs upregulated by 5-Aza-CdR and PBA in AGS and T24 cells (microarray analysis). Ratio represents signal ratio of 5-Aza-CdR and PBA treatment compared with no treatment. Presence of Alu repeats in the upstream region of each miRNA is indicated by filled box. The expression profile of T24 is modified from Figure 1a of the reference (Saito *et al.*, 2006). (**b**) Quantitative reverse transcriptase (RT)–PCR analyses of Alu-associated miRNAs in AGS cells not treated (NT, blank bar) or treated with 5-Aza-CdR and PBA (AP, filled bar). The expression level was normalized to the U6 RNA expression level and expressed as mean + s.d. (**c**) Quantitative RT–PCR analyses of *miR-512-5p* and *miR-517b* in TMK1 and MKN45 cells not treated (NT, blank bar) or treated with 5-Aza-CdR and PBA (AP, filled bar). The expression level was normalized to the U6 RNA expression level and expressed as mean + s.d.

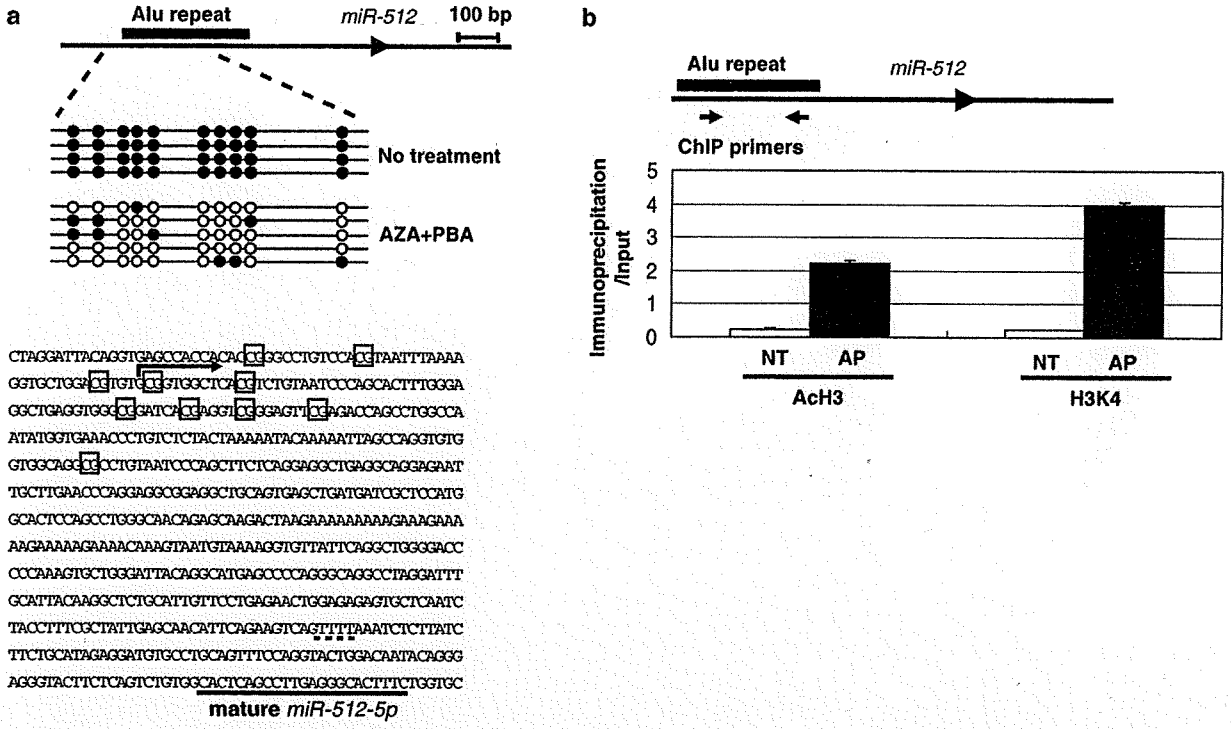

Figure 2 Alterations in DNA methylation and histone modification at Alu repeats of *miR-512* in AGS cells after epigenetic treatment. (a) DNA methylation status of CpG sites (shown as boxes) around the promoter region of *miR-512-5p* in AGS cells not treated or treated with 5-aza-2′-deoxycytidine (5-Aza-CdR) and 4-phenylbutyric acid (PBA) was determined by bisulfite genomic sequencing. Blank circle, unmethylated CpG; filled circle, methylated CpG. The bent arrow indicates the putative transcriptional start site of *miR-512-5p* determined by 5′ RACE assay. Note that Alu elements are separated from mature *miR-512-5p* sequences by Pol III terminator (TTTT, dot line), indicating that Pol III at Alu elements cannot transcribe *miR-512-5p*. (b) The levels of acetylated histone H3 (AcH3) and dimethylated histone H3-K4 (H3K4) of *miR-512-5p* were determined by chromatin immunoprecipitation (ChIP) assay in AGS cells not treated (NT, blank bar) or treated with 5-Aza-CdR and PBA (AP, filled bar). Immunoprecipitation/Input = (immunoprecipitated DNA with each antibody −No Antibody Control (NAC))/(input DNA−NAC). Values are expressed as mean + s.d.

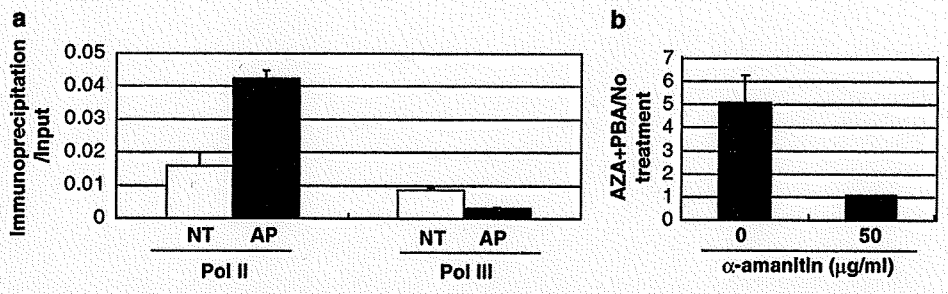

Figure 3 Activation of *miR-512-5p* by epigenetic treatment is mediated by Pol II. (a) Levels of Pol II and Pol III around the promoter regions of *miR-512-5p* were determined by chromatin immunoprecipitation assay in AGS cells not treated (NT, blank bar) or treated with 5-aza-2′-deoxycytidine (5-Aza-CdR) and 4-phenylbutyric acid (PBA) (AP, filled bar). Immunoprecipitation/Input = (immunoprecipitated DNA with each antibody −No Antibody Control (NAC))/(input DNA−NAC). Values are expressed as mean + s.d. (b) AGS cells treated with 5-Aza-CdR and PBA were incubated in 0 or 50 μg/ml of α-amanitin for 7 h before the cells were harvested for assay. Ratios of 5-Aza-CdR and PBA treatment compared with no treatment in expression levels of *miR-512-5p* normalized with U6 were shown. Values are expressed as mean + s.d.

Activation of miR-512-5p *by epigenetic treatment is mediated by Pol II*

To assess whether epigenetic activation of *miR-512-5p* is mediated by Pol II or Pol III, we have carried out ChIP assay of Pol II and Pol III on the promoter region of *miR-512-5p* in AGS cells (Figure 3a). The results of ChIP assay show that Pol II signal at Alu repeats is significantly increased after epigenetic treatment, whereas Pol III signal shows no increase. Pol II is highly sensitive to α-amanitin and therefore treatment of

mammalian cells with α-amanitin at a concentration of 50 μg/ml for 5–9 h results in the selective inhibition of Pol II. AGS cells with epigenetic treatment were incubated in 0 or 50 μg/ml of α-amanitin for 7 h before the cells were harvested for assay. As shown in Figure 3b, we have found that the epigenetic activation of *miR-512-5p* is inhibited by α-amanitin treatment. In addition, we have identified the putative Pol II transcriptional start site of *miR-512-5p* by 5′-rapid amplification of cDNA ends (5′-RACE) (Figure 2a). These findings indicate that activation of *miR-512-5p* by epigenetic treatment is mediated by Pol II.

Overexpression of miR-512-5p *suppresses* Mcl-1 *and induces apoptosis*

Identification of target genes of Alu-associated miRNAs is essential to investigate their biological function. Recent studies have shown that miRNAs can regulate expression of their target genes by decreasing mRNA stability, in addition to translational inhibition (Yekta *et al*., 2004; Bagga *et al*., 2005; Wu *et al*., 2006). The strategy to identify target genes of *miR-512-5p* is shown in Figure 4a. First of all, we conducted a microarray analysis to screen for genes that were threefold downregulated by treatment with 5-Aza-CdR and PBA, because target genes of *miR-512-5p* were expected to be suppressed by overexpression of *miR-512-5p*. Then, we identified 69 genes, which are known to be involved in cell proliferation, apoptosis and differentiation. We finally selected nine genes as potential target genes of *miR-512-5p* by referring to the database for the prediction of miRNA targets (microRNA.org, http://www.microrna.org). Among these nine genes, we especially focused on well-known oncogenes, *Jun* and *Mcl-1*. To confirm that *Jun* and *Mcl-1* are target genes of *miR-512-5p*, AGS cells were transfected with *miR-512-5p* precursor molecules, and the expression levels of *Jun* and *Mcl-1* were assessed by quantitative RT–PCR. As shown in Figure 4b, significant downregulation of *Jun* and *Mcl-1* was observed in AGS cells after transfection of *miR-512-5p*. As the expression of *Mcl-1* was remarkably downregulated by overexpression of *miR-512-5p*, we further examined expression level of Mcl-1 by western blotting. The expression level of Mcl-1 was significantly downregulated in AGS cells both after

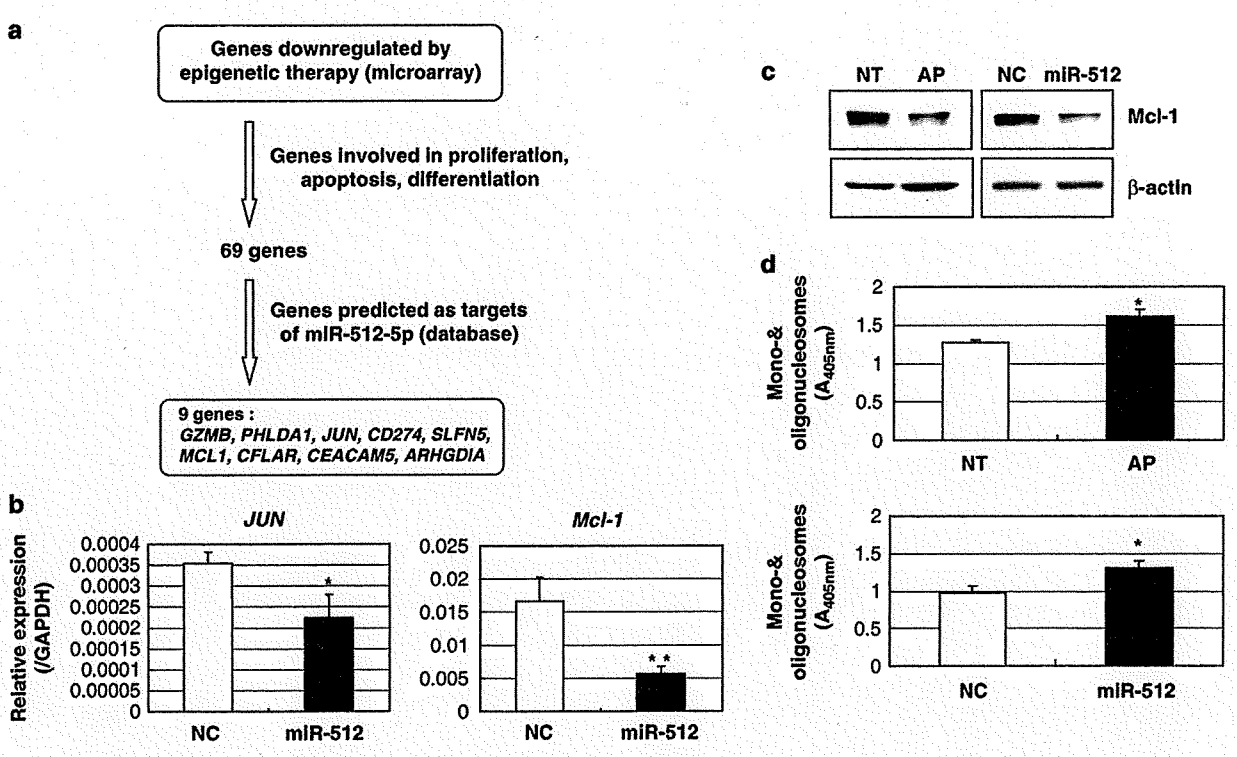

Figure 4 Overexpression of *miR-512-5p* induces suppression of *Mcl-1* and apoptosis. (**a**) A schema to identify targets of *miR-512-5p* using the microarray data of AGS cells treated with 5-aza-2′-deoxycytidine (5-Aza-CdR) and 4-phenylbutyric acid (PBA) and the database for the prediction of miRNA targets. (**b**) mRNA expression of *Jun* and *Mcl-1* in AGS cells transfected with *miR-512-5p* precursor molecules (miR-512) and negative control (NC) was analysed by quantitative reverse transcriptase–PCR. The expression level was normalized to the *GAPDH* RNA expression level and expressed as mean + s.d. $*P<0.05$, $**P<0.01$ compared with negative control. (**c**) The protein expression level of Mcl-1 was analysed by western blotting in AGS cells not treated (NT) or treated with 5Aza-CdR and PBA (AP), as well as in AGS cells transfected with *miR-512-5p* precursor molecules (miR-512) and negative control (NC). β-actin is used as a loading control. (**d**) Levels of cytoplasmic histone-associated DNA fragments (mono- and oligonucleosomes) in AGS cells after transfection of *miR-512-5p* and after treatment with 5-Aza-CdR and PBA. Values are expressed as mean + s.d. $*P<0.05$ compared with negative control or untreated cells. GAPDH, glyceraldehydes 3-phosphate dehydrogenase.

treatment with 5-Aza-CdR and PBA and after transfection of *miR-512-5p* (Figure 4c).

In addition, levels of apoptosis were evaluated by photometric enzyme-immunoassay for the detection of cytoplasmic histone-associated DNA fragments. Significant increase of the levels of cytoplasmic histone-associated DNA fragments (mono- and oligonucleosomes) was observed in AGS cells both after treatment with 5-Aza-CdR and PBA and after transfection of *miR-512-5p* (Figure 4d).

To further confirm target specificity between *miR-512-5p* and its potential target, *Mcl-1*, we carried out luciferase reporter assay with a vector containing the putative *Mcl-1* 3′ untranslated region (UTR) target site downstream of the luciferase reporter gene, which was transfected into AGS cells. Base pairing between *miR-512-5p* and wild-type (WT) or mutant (MUT) target site in the 3′ UTR of *Mcl-1* mRNA is shown in Figure 5a. Luciferase activities of AGS cells transfected with Mcl-1-WT construct were significantly lower after epigenetic treatment and after transfection of *miR-512-5p*, whereas those with Mcl-1-MUT construct showed no significant difference (Figure 5b). These data suggest that *Mcl-1* is one of the targets of *miR-512-5p* and that activation of *miR-512-5p* induces suppression of *Mcl-1*, resulting in apoptosis of gastric cancer cells.

Discussion

Alu repeats are the most frequent repetitive elements in the human genome and have been considered as 'junk DNA' with no important function. However, Borchert *et al.* (2006) have shown that Alu repeats in the miRNA cluster on chromosome 19 can function as Pol III promoters of downstream miRNAs. These Alu-associated miRNAs are shown to be silenced in the human tissues except the placenta (Bentwich *et al.*, 2005). We also found that Alu-associated miRNAs are silenced in both gastric cancers and non-cancerous mucosae (data not shown).

In this study, we show that one of the Alu-associated miRNAs, *miR-512-5p*, is silenced by epigenetic mechanisms, and that chromatin remodeling at Alu repeats by DNA methylation inhibitors and HDAC inhibitors can activate expression of silenced *miR-512-5p* in human gastric cancer cells. The DNA demethylating agent 5-Aza-CdR and HDAC inhibitor PBA were effective at reducing DNA methylation level and activating chromatin structure at the promoter region of *miR-512-5p*. In agreement with our results, earlier studies have suggested that Alu transcription is regulated by epigenetic mechanisms such as DNA methylation and histone modification at Alu repeats (Liu *et al.*, 1994; Kondo and Issa, 2003).

Although it has been reported that Alu-associated miRNAs are transcribed by Pol III (Borchert *et al.*, 2006), our results suggest that epigenetic activation of *miR-512-5p* is mediated by Pol II. Interestingly, Alu elements on the promoter region of *miR-512-5p* are separated from mature *miR-512-5p* sequences by Pol III terminator (TTTT), indicating that Pol III at Alu elements cannot transcribe *miR-512-5p* (Figure 2a). This finding supports our results that chromatin remodeling by epigenetic treatment at Alu repeats can activate *miR-512-5p* through Pol II. A recent study also reports about Pol II transcription associated with Alu repeats and CpG islands in human promoters (Oei *et al.*, 2004).

Gastric cancer is the second most common cause of cancer-related death worldwide. Although the incidence of gastric cancer has declined in western countries, it remains a major health problem throughout the rest of the world, especially in China and Japan (Parkin, 2001).

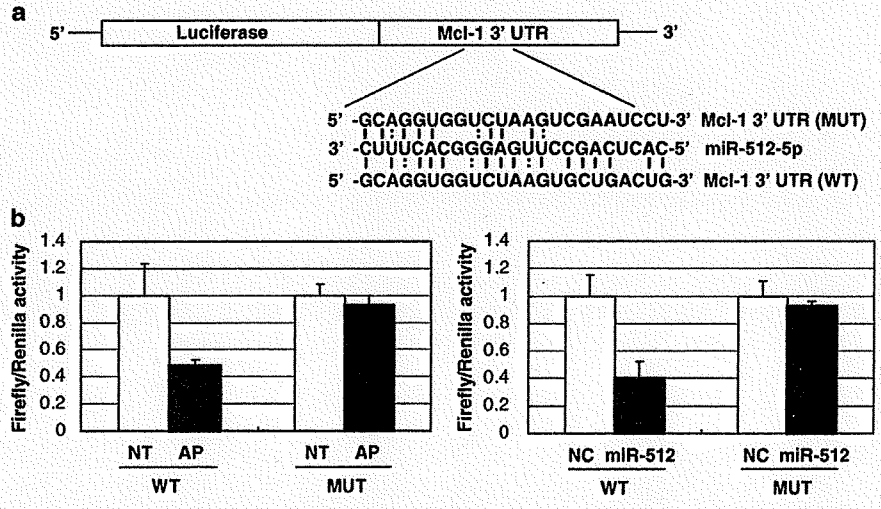

Figure 5 Identification of *Mcl-1* as a target of *miR-512-5p*. (**a**) Luciferase reporter constructs containing wild-type (WT) or mutant (MUT) target site of the 3′ untranslated region (UTR) of *Mcl-1* mRNA. (**b**) The firefly luciferase activity normalized to the *Renilla* luciferase activity in AGS cells not treated (NT) or treated with 5-aza-2′-deoxycytidine and 4-phenylbutyric acid (AP) and in AGS cells transfected with negative control (NC) or *miR-512-5p* precursor molecules (miR-512).

For gastric cancer that is diagnosed at an advanced stage, systemic chemotherapy is the only treatment available, besides supportive care. The *Mcl-1* gene is a member of the *Bcl-2* family and an anti-apoptotic protein originally isolated from the ML-1 human myeloid leukemia cell line during cell differentiation (Kozopas *et al.*, 1993). The biological relevance of Mcl-1 as an anti-apoptotic protein promoting cell survival has been reported in various human malignancies (Zhou *et al.*, 1997; Shigemasa *et al.*, 2002; Taniai *et al.*, 2004). Elevated expression of *Mcl-1* and its association with poor prognosis have been reported in gastric cancer (Krajewska *et al.*, 1996; Maeta *et al.*, 2004). Interestingly, Wacheck *et al.* (2006) have proposed *Mcl-1* antisense therapy as a promising approach for the treatment of gastric cancer. They have shown that downregulation of *Mcl-1* by antisense therapy produced a significant increase in apoptosis and a decrease in cell growth, and that the combination of *Mcl-1* antisense oligonucleotide and anti-cancer agents, such as docetaxel and cisplatin, showed synergistic chemopreventive activity (Wacheck *et al.*, 2006; Zangemeister-Wittke and Huwiler, 2006). Our results show that activation of *miR-512-5p* induced by chromatin-modifying drugs suppresses *Mcl-1*, resulting in apoptosis of gastric cancer cells. In addition, activation of Alu-associated miRNAs by epigenetic treatment seems to be more specific in gastric cancer cells compared with bladder cancer cells. These results indicate that Alu-associated miRNAs could be novel therapeutic targets of human gastric cancer.

In conclusion, our results suggest that chromatin remodeling at Alu repeats by DNA demethylation and HDAC inhibition can induce expression of silenced miRNAs, which can serve as 'endogenous silencers' of target oncogenes in gastric cancer cells. As there is a possibility that other proteins activated by epigenetic treatment may also contribute to apoptosis in gastric cancer cells, further studies are necessary to verify whether activation of Alu-associated miRNAs by epigenetic therapy could be an effective approach for the prevention and treatment of human gastric cancer.

Materials and methods

Cell lines and epigenetic treatment
The AGS, MKN45 and TMK1 human gastric cancer cell lines were used. AGS was obtained from the American Type Culture Collection (Rockville, MD, USA), and MNK45 was obtained from the Japan Health Science Foundation (Osaka, Japan). TMK1 is a generous gift from Dr Wataru Yasui (Ochiai *et al.*, 1985). Cells were cultured in RPMI1640 medium supplemented with 10% fetal bovine serum. They were seeded at 24 h before treatment with 5-Aza-CdR (Sigma-Aldrich, St Louis, MO, USA) and PBA (Sigma-Aldrich). 5-Aza-CdR was removed after 24 h, whereas the cells were continuously exposed to PBA for 96 h.

RNA extraction and microarray analyses
Total RNA, including small RNA, was extracted using the mirVana miRNA isolation kit (Ambion, Austin, TX, USA). miRNA microarray analysis was carried out by LC Sciences (www.lcsciences.com, Houston, TX, USA), and gene expression profile was analysed using the whole human genome oligo microarray kit (Agilent technologies, Santa Clara, CA, USA). All data were submitted to the ArrayExpress database, and the accession numbers are E-MEXP-1820 and E-MEXP-1821, respectively.

Quantitative RT–PCR of miRNAs
MicroRNA expression levels were analysed by quantitative RT–PCR using the TaqMan microRNA assay for *miR-512-5p, -515-5p, -517b, -518b* and *-526b* (Applied Biosystems, Foster City, CA, USA), in accordance with the manufacturer's instructions.

Bisulfite genomic sequencing
Genomic DNA was converted with sodium bisulfite. After amplification of the bisulfite-converted DNA by nested PCR with specific primers for *miR-512*, DNA methylation levels were analysed by bisulfite genomic sequencing as described earlier (Saito *et al.*, 2006). The sequences of the primers used are listed in Supplementary Table 1.

Chromatin immunoprecipitation assay
The ChIP assay was carried out as described earlier (Saito *et al.*, 2006). Antibodies to dimethylated histone H3-K4 (Upstate, Temecula, CA, USA), acetylated histone H3 (Upstate), Pol II (Upstate) and Pol III (anti-RPC 53, see Acknowledgements) were used. Quantitative analysis was carried out by real-time PCR with the CYBR Premix Ex Taq (Takara Bio, Ohtsu, Japan) using the Thermal Cycler Dice Real-Time System (Takara Bio). The sequences of the primers used are listed in Supplementary Table 1. The fraction of immunoprecipitated DNA was calculated as follows: (immunoprecipitated DNA with each antibody−nonspecific antibody control (NAC))/(input DNA−NAC).

5′-Rapid amplification of cDNA ends
5′ ends of mRNA were detected using the RLM-RACE kit (Ambion) according to the manufacturer's protocols. The inner 5′ RLM-RACE PCR products were cut from 2% agarose gel, purified using Gel Extraction Kit (Qiagen, Tokyo, Japan) and sequenced with an inner gene-specific primer. The sequences of the primers used are listed in Supplementary Table 1.

Western blotting and quantitative RT–PCR
Protein extracts were separated by SDS/polyacrylamide gel electrophoresis and transferred onto a nitrocellulose membrane. Membranes were hybridized with antibodies against Mcl-1 (S-19, Santa Cruz Biotechnology, Santa Cruz, CA, USA).

Total RNA was used for reverse transcription. After incubation with DNase I (Promega, Madison, WI, USA) to eliminate DNA contamination, Superscript III (Invitrogen, Carlsbad, CA, USA) and random hexamers (Invitrogen) were added for first-strand cDNA synthesis, then, quantitative PCR was carried out with primers specific for *Jun* and *Mcl-1* (Supplementary Table 1).

Transfection of miR-512-5p *precursor molecules*
The *miR-512-5p* precursor molecules and negative control 1 precursor miRNAs were purchased from Ambion. They were transfected into AGS cells at a final concentration of 100 nM each using oligofectamine (Invitrogen), in accordance with the manufacturer's instructions. At 48 h after transfection, cells were collected and the expression of Mcl-1 was analysed by western blotting as described above.

Apoptosis assay
AGS cells were transfected with *miR-512-5p* and negative control or treated with 5-Aza-CdR and PBA. Forty-eight hours later, apoptosis was evaluated by photometric enzyme-immunoassay for the detection of cytoplasmic histone-associated DNA fragments using the Cell Death Detection ELISA kit (Roche, Mannheim, Germany) (Suzuki *et al.*, 1998).

Luciferase assay
Luciferase constructs were made by ligating oligonucleotides containing the wild-type or mutant target site of the *Mcl-1* 3′ UTR into the *Xba* I site of the pGL3-control vector (Promega, Figure 5a). AGS cells were transfected with 0.4 μg of firefly luciferase reporter vector containing wild-type or mutant target site and 0.02 μg of the control vector containing *Renilla* luciferase, pRL-CMV (Promega), using lipofectamine 2000 (Invitrogen) in 24-well plates. Luciferase assays were carried out at 48 h after transfection using the Dual Luciferase Reporter Assay System (Promega). Firefly luciferase activity was normalized to *Renilla* luciferase activity.

Conflict of interest

Dr Saito's work has been funded by a Grant-in-Aid for Scientific Research from the Japan Society for the Promotion of Science (JSPS). Dr Suzuki's work has been funded by a Grant-in-Aid for Exploratory Research from the JSPS. Dr Kanai's work has been funded by the Ministry of Health, Labor and Welfare of Japan. Dr Hibi's work has been funded by the JSPS and the Ministry of Education, Culture, Sports, Science and Technology.

Acknowledgements

The authors are grateful to Dr Robert Roeder at Rockefeller University for providing antibody to Pol III. This work was supported by a Grant-in-Aid for Scientific Research C from the Japan Society for the Promotion of Science (JSPS) (19599024, to Y.S.) and a Grant-in-Aid for Exploratory Research from JSPS (19659057, to HS).

References

Bagga S, Bracht J, Hunter S, Massirer K, Holtz J, Eachus R *et al.* (2005). Regulation by let-7 and lin-4 miRNAs results in target mRNA degradation. *Cell* **122**: 553–563.

Bentwich I, Avniel A, Karov Y, Aharonov R, Gilad S, Barad O *et al.* (2005). Identification of hundreds of conserved and nonconserved human microRNAs. *Nat Genet* **37**: 766–770.

Borchert GM, Lanier W, Davidson BL. (2006). RNA polymerase III transcribes human microRNAs. *Nat Struct Mol Biol* **13**: 1097–1101.

Calin GA, Croce CM. (2006a). MicroRNA signatures in human cancers. *Nat Rev Cancer* **6**: 857–866.

Calin GA, Croce CM. (2006b). MicroRNAs and chromosomal abnormalities in cancer cells. *Oncogene* **25**: 6202–6210.

Esteller M. (2002). CpG island hypermethylation and tumor suppressor genes: a booming present, a brighter future. *Oncogene* **21**: 5427–5440.

Gal-Yam EN, Saito Y, Egger G, Jones PA. (2008). Cancer epigenetics: modifications, screening, and therapy. *Annu Rev Med* **59**: 267–280.

Kondo Y, Issa JP. (2003). Enrichment for histone H3 lysine 9 methylation at Alu repeats in human cells. *J Biol Chem* **278**: 27658–27662.

Kozopas KM, Yang T, Buchan HL, Zhou P, Craig RW. (1993). MCL1, a gene expressed in programmed myeloid cell differentiation, has sequence similarity to BCL2. *Proc Natl Acad Sci USA* **90**: 3516–3520.

Krajewska M, Fenoglio-Preiser CM, Krajewski S, Song K, Macdonald JS, Stemmerman G *et al.* (1996). Immunohistochemical analysis of Bcl-2 family proteins in adenocarcinomas of the stomach. *Am J Pathol* **149**: 1449–1457.

Liu WM, Maraia RJ, Rubin CM, Schmid CW. (1994). Alu transcripts: cytoplasmic localisation and regulation by DNA methylation. *Nucleic Acids Res* **22**: 1087–1095.

Maeta Y, Tsujitani S, Matsumoto S, Yamaguchi K, Tatebe S, Kondo A *et al.* (2004). Expression of Mcl-1 and p53 proteins predicts the survival of patients with T3 gastric carcinoma. *Gastric Cancer* **7**: 78–84.

Ochiai A, Yasui W, Tahara E. (1985). Growth-promoting effect of gastrin on human gastric carcinoma cell line TMK-1. *Jpn J Cancer Res* **76**: 1064–1071.

Oei SL, Babich VS, Kazakov VI, Usmanova NM, Kropotov AV, Tomilin NV. (2004). Clusters of regulatory signals for RNA polymerase II transcription associated with Alu family repeats and CpG islands in human promoters. *Genomics* **83**: 873–882.

Parkin DM. (2001). Global cancer statistics in the year 2000. *Lancet Oncol* **2**: 533–543.

Saito Y, Jones PA. (2006). Epigenetic activation of tumor suppressor microRNAs in human cancer cells. *Cell Cycle* **5**: 2220–2222.

Saito Y, Liang G, Egger G, Friedman JM, Chuang JC, Coetzee GA *et al.* (2006). Specific activation of microRNA-127 with down-regulation of the proto-oncogene BCL6 by chromatin-modifying drugs in human cancer cells. *Cancer Cell* **9**: 435–443.

Shigemasa K, Katoh O, Shiroyama Y, Mihara S, Mukai K, Nagai N *et al.* (2002). Increased MCL-1 expression is associated with poor prognosis in ovarian carcinomas. *Jpn J Cancer Res* **93**: 542–550.

Suzuki H, Seto K, Mori M, Suzuki M, Miura S, Ishii H. (1998). Monochloramine induced DNA fragmentation in gastric cell line MKN45. *Am J Physiol* **275**: G712–G716.

Taniai M, Grambihler A, Higuchi H, Werneburg N, Bronk SF, Farrugia DJ *et al.* (2004). Mcl-1 mediates tumor necrosis factor-related apoptosis-inducing ligand resistance in human cholangiocarcinoma cells. *Cancer Res* **64**: 3517–3524.

Wacheck V, Cejka D, Sieghart W, Losert D, Strommer S, Crevenna R *et al.* (2006). Mcl-1 is a relevant molecular target for antisense oligonucleotide strategies in gastric cancer cells. *Cancer Biol Ther* **5**: 1348–1354.

Wu L, Fan J, Belasco JG. (2006). MicroRNAs direct rapid deadenylation of mRNA. *Proc Natl Acad Sci USA* **103**: 4034–4039.

Yekta S, Shih IH, Bartel DP. (2004). MicroRNA-directed cleavage of HOXB8 mRNA. *Science* **304**: 594–596.

Yoo CB, Jones PA. (2006). Epigenetic therapy of cancer: past, present and future. *Nat Rev Drug Discov* **5**: 37–50.

Zangemeister-Wittke U, Huwiler A. (2006). Antisense targeting of Mcl-1 has therapeutic potential in gastric cancer. *Cancer Biol Ther* **5**: 1355–1356.

Zhou P, Qian L, Kozopas KM, Craig RW. (1997). Mcl-1, a Bcl-2 family member, delays the death of hematopoietic cells under a variety of apoptosis-inducing conditions. *Blood* **89**: 630–643.

Supplementary Information accompanies the paper on the Oncogene website (http://www.nature.com/onc)

Cancer Science
The official journal of the Japanese Cancer Association JCA

Characteristics of prostate cancers found in specimens removed by radical cystoprostatectomy for bladder cancer and their relationship with serum prostate-specific antigen level

Tohru Nakagawa,[1,3] Yae Kanai,[2] Motokiyo Komiyama,[1] Hiroyuki Fujimoto[1] and Tadao Kakizoe[1]

[1]Urology Division, National Cancer Center Hospital; [2]Pathology Division, National Cancer Center Research Institute, Tokyo, Japan

(Received April 13, 2009/Revised June 18, 2009/Accepted June 22, 2009/Online publication July 30, 2009)

Prostate cancer mass screening using serum prostate-specific antigen (PSA) has been conducted widely in the world. However, little is known about the true prevalence of prostate cancer in the 'normal' PSA range (4.0 ng/mL or less). The aim of the present study was to elucidate the clinicopathological features of prostate cancer occurring in men with a wide range of PSA levels. The study comprised 349 male patients who underwent radical cystoprostatectomy for bladder cancer. Patients who had had treatment for known prostate cancer were excluded. Tissue specimens were reviewed microscopically. Ninety-one patients (26.1%) were found to have prostate cancer, and 68 (74.7%) of these 91 cancers were considered to be clinically significant. Both increasing patient age and PSA level were significantly correlated with an increased incidence of both all and significant prostate cancers. Sixty-five (21.9%) among 297 patients with PSA < 4.0 ng/mL had prostate cancer, and 45 (69.2%) of the 65 cancers were significant cancers. Eighteen patients had prostate cancers 0.5 mL or more in volume. Among the 18 patients, the PSA level was 4 ng/mL or more in 11, and 3 ng/mL or more in 15. Our study shows that prostate cancer is a common finding in radical cystoprostatectomy specimens excised because of bladder cancers, and a significant proportion of these cancers are clinically significant. PSA still appears to be a useful screening tool for detecting prostate cancers with significant volume. (*Cancer Sci* 2009; 100: 1880–1884)

Prostate cancer is one of the leading causes of mortality and morbidity in developed countries.[1] Screening of serum PSA followed by systematic prostate biopsy has enabled detection of prostate cancer at an earlier stage,[2] although it is still debatable whether mass screening using PSA contributes significantly to reduction in mortality from prostate cancer.[3]

Historically, 4.0 ng/mL PSA has been used as the threshold to prompt prostate biopsy. Although it is known that prostate cancers do exist even in the low PSA range (4.0 ng/mL or less),[4] until recently little was known about the true prevalence of prostate cancer in the low PSA range because most men in this category do not undergo prostate biopsy.[5] In 2004, Thompson *et al.* reported data from the PCPT showing that biopsy-detectable prostate cancer is not rare among men with a low PSA level (4.0 ng/mL or less).[6] This result provoked a discussion about the optimal threshold of PSA for recommending biopsy, although no definitive agreement has been reached so far.[7,8] Although the PCPT demonstrated the prevalence of biopsy-detectable prostate cancer in the low PSA range, there is still a notable lack of data based on thorough histological evaluation of the whole prostate in relation to PSA level in a large general population.

It is possible to microscopically examine the whole prostate of autopsied individuals in whom prostate cancer had not been suspected before death.[9] Although most latent prostate cancers observed in autopsy cases are small lesions, their histology is not different from clinical cancers, and they may be merely in the early phase of progression.[10,11] Usually, however, PSA levels are not available in autopsy cases.

Radical cystoprostatectomy (RCP) is a gold-standard treatment for invasive bladder cancer.[12] Even though some researchers have reported an epidemiological association between bladder cancer and prostate cancer,[13] the specimen obtained from this operation represents a fairly random sample of whole prostate tissue from asymptomatic men. Several studies have examined the incidence and histopathological characteristics of prostate cancer found incidentally in RCP specimens.[14–18] They showed that incidental prostate cancer is not rare in RCP specimens (incidence, 4–60%).[14–18] However, only a few of them examined its relationship with PSA value.[15–18]

In order to elucidate the incidence and histopathological features of prostate cancers occurring in men with a wide range of PSA levels, we reviewed 349 whole prostate tissues in RCP specimens excised because of bladder cancer in Japanese men.

Patients and Methods

Medical records of 354 consecutive men who underwent RCP for bladder cancer at the National Cancer Center Hospital between July 1995 and April 2008 were reviewed retrospectively. The study was approved by the institutional review board.

Three men were excluded from the study because they had undergone pelvic irradiation for bladder cancer before RCP. Two were also excluded because they had been diagnosed as having prostate cancer and treated with androgen ablation and/or radiation therapy before RCP. Thus, 349 men were included in the present study.

A routine pathological examination was conducted on all RCP specimens by sectioning the prostate and bladder every 5 mm. A single pathologist (YK) reviewed the specimens microscopically. Each prostate cancer was staged and graded based on the 2002 International Union Against Cancer (UICC) TNM system[19] and 2005 modified International Society of Urological Pathology (ISUP) Gleason grading system.[20] Tumor volume was calculated using the formula:

$$\text{volume} = (\text{width} \times \text{height} \times \text{length}) \times \pi/6 \times 1.5,$$

in which length is calculated from 0.5 cm multiplied by the number of slices containing tumors and 1.5 is a tissue shrinkage factor.[21]

[3]To whom correspondence should be addressed. E-mail: trnakaga@ncc.go.jp

doi: 10.1111/j.1349-7006.2009.01267.x

Table 1. Status and pathology of prostate biopsy and prostate-specific antigen (PSA) levels before radical cystoprostatectomy (RCP) in the 349 patients

PSA	Prostate biopsy before RCP		
	Yes		No biopsy
	Prostate cancer proved	Benign prostatic tissue	
<4 ng/mL	1	0	296
≥4 ng/mL	3	2	44
Unknown	0	0	3

Table 2. Characteristics of prostate cancers found in radical cystoprostatectomy specimens

Characteristic	Patients	
	n	%
Gleason score		
6 or less	24	26.4
7 (3 + 4)	54	59.3
7 (4 + 3)	9	9.9
8–10	4	4.4
pT stage		
pT2	85	93.4
pT3a	3	3.3
pT3b	1	1.1
pT4	2	2.2
Lymph node status		
pN0	89	97.8
pN1	1	1.1
pN2	1	1.1
Surgical margin status		
Not involved by tumor	87	95.6
Involved by tumor	4	4.4
Perineural invasion		
Negative	69	75.8
Positive	22	24.2

The serum PSA level was determined routinely before RCP at the outpatient clinic. Measurement of PSA levels was carried out using the Delfia-PSA assay (Pharmacia Diagnostics Co., Tokyo, Japan) until September 1997, the Lumipulse PSA assay (Fujirebio, Tokyo, Japan) until July 2004, and the Lumipulse PSA-N assay (Fujirebio) thereafter.

Correlations of clinicopathological parameters between groups were analyzed by Mann–Whitney *U*-test or Kruskal–Wallis test. Differences with *P*-values < 0.05 were considered significant.

Results

The median patient age was 65 years (range, 27–89 years). Preoperative PSA levels were not evaluated in 3 of the 349 men. The median preoperative PSA level was 1.28 ng/mL (range, 0.03–20.603 ng/mL) for the 346 patients.

In 6 of the 349 patients, prostate biopsy had been carried out before RCP. The presence or absence of prostate biopsy, pathology of the biopsy specimen, and serum PSA levels in the 349 patients are summarized in Table 1.

Ninety-one patients (26.1%) were found to have prostate cancer. Of these, four (1.1%) had been preoperatively diagnosed as having prostate cancer by needle biopsy, but had not been treated before RCP. Eighty-seven (24.9%) were found to have incidental prostate cancer.

The pathological features of these 91 prostate cancers are shown in Table 2. The distribution of the prostate cancer volumes

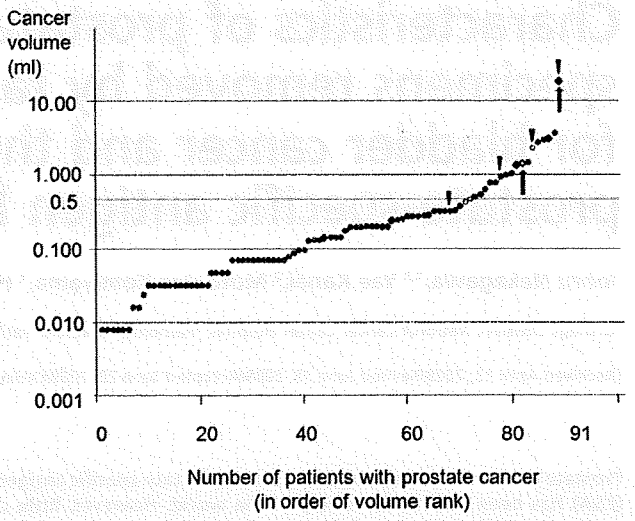

Fig. 1. Volume distribution of prostate cancers. All 91 prostate cancers are plotted in order of volume rank. Each circle and square indicates one prostate cancer. Squares indicate pT3 or pT4 cancers. Clear circles and squares indicate cancers diagnosed by biopsy before cystoprostatectomy. Arrowheads indicate cancers with a Gleason score of 8 or more. Arrows indicate cancers with lymph node metastasis.

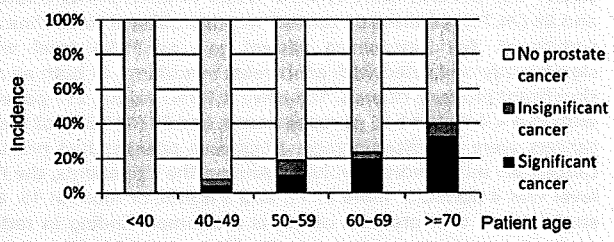

	<40	40–49	50–59	60–69	>=70
Number of patients	6	25	80	128	110
All prostate cancer	0	2	15	30	44
	0%	8.0%	18.8%	23.4%	40%
Significant cancer	0	1	8	24	35
	0%	4.0%	10.0%	18.8%	31.8%

Fig. 2. Incidence of prostate cancer in each age group. The definition of significant cancer is given in the Results section.

is shown in Figure 1. Larger cancers were more likely to have a higher Gleason score and to have lymph node metastasis (Fig. 1). As for the relationship between cancer volume and pT stage, even small cancers could be at high pT stage: a cancer 0.23 mL in volume showed extracapsular extension (pT3a). A cancer 0.13 mL in volume arose in the prostatic base and invaded to the bladder neck (pT4).

The incidence of prostate cancer increased with patient age (Fig. 2). The median age of the patients with prostate cancer was 69 years (range, 43–81 years), and was significantly higher than that of patients without prostate cancer (median, 63.5 years; range, 27–89 years) ($P < 0.0001$, Mann–Whitney *U*-test).

The incidence of prostate cancer increased with the PSA level (Fig. 3). The median PSA level in the patients with prostate cancer was 1.90 ng/mL (range, 0.26–20.60) and was significantly higher than in those without prostate cancer (median 1.20 ng/mL, range 0.03–13.27 ng/mL) ($P < 0.0001$, Mann–Whitney *U*-test).

Prostate cancer was considered clinically significant if any of the following criteria were present: total tumor volume ≥ 0.5 mL,

Table 3. Relationship between prostate cancer and patient age

Prostate cancer	No. patients	Median age (years)	P-value			
No prostate cancer	258	63.5 (range 27–89)	$P < 0.0001$*			
Prostate cancer	91	69 (range 43–81)		$P = 0.2340$*	$P < 0.0001$†	$P < 0.0001$*
Insignificant	23	67 (range 43–78)				
Significant	68	70 (range 46–81)		$P = 0.1216$*		

*Mann–Whitney *U*-test, †Kruskal–Wallis test.

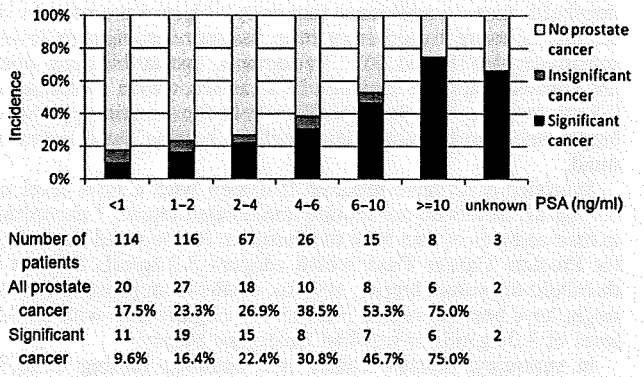

Fig. 3. Incidence of prostate cancer in each prostate-specific antigen (PSA) range. Definition of significant cancer is given in the Results section.

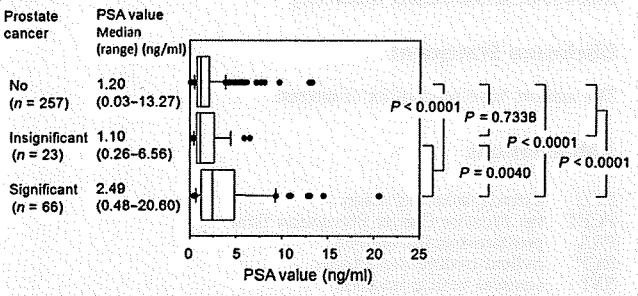

Fig. 4. Relationship between prostate cancer and prostate-specific antigen (PSA) value. The boxes show a range of 25–75 percentiles, and the whiskers a range of 10–90 percentiles. The vertical bars in each box indicate median values. Correlation was calculated using the Mann–Whitney *U*-test.

Gleason grade ≥ 4, ECE, SVI, or lymph node metastasis. Sixty-eight patients (74.7%) had significant prostate cancer. The reasons for designating these cancers as 'significant' were: tumor volume ≥ 0.5 mL in 18 patients (19.8%), Gleason grade ≥ 4 in 67 patients (73.6%), ECE in five patients (5.5%), SVI in one patient (1.1%), and lymph node metastasis in two patients (2.2%).

The incidence of significant prostate cancer increased with patient age (Fig. 2). The median age of the patients with significant prostate cancer was 70 years (range, 46–81 years), and was significantly higher than that of patients without significant prostate cancer (median, 64 years; range, 27–89 years) ($P < 0.0001$, Mann–Whitney *U*-test) (Table 3).

The incidence of significant prostate cancer increased with the PSA level (Fig. 3). Figure 4 shows the distribution of PSA levels in the patients with significant, insignificant, or no prostate cancer. The median PSA level in the patients with significant prostate cancer was 2.49 ng/mL (range, 0.48–20.60 years) and was significantly higher than in those with insignificant cancer (median, 1.10 ng/mL; range, 0.26–6.56 ng/mL) ($P = 0.0040$) and in those without cancer (median, 1.20 ng/mL; range 0.03–13.27 ng/mL) ($P < 0.0001$). The PSA level in the patients with insignificant prostate cancer was not significantly different from that in patients without cancer ($P = 0.7338$) (Fig. 4).

The median follow-up period was 36 months (range, 1–128 months) for the 91 patients with prostate cancer. None of the patients died of prostate cancer during follow-up. One patient, who had a preoperative PSA level of 5.0 ng/mL and a Gleason grade 4 + 3 prostate cancer 2.96 mL in volume, developed biochemical recurrence (PSA recurrence; PSA > 0.2 ng/mL) at 36 months after surgery without any detectable mass lesion. His serum PSA level was 0.583 ng/mL, and no additional therapy has yet been started at 42 months of follow-up.

Discussion

The incidence of prostate cancer varies among races; East Asians have a lower cumulative incidence than white and black people in the USA and Europe.[22] However, the incidence of latent prostate cancer does not differ between Japanese and white and black people in the USA.[9] Latent cancer is not different from clinical cancer in terms of histology.[10,11] The proportion of Japanese men who undergo PSA screening remains at only 5%,[23] whereas 75% of men aged 50 years or older have had a PSA test in the USA.[24] In Japan, however, the morbidity and mortality of prostate cancer have been increasing,[22] and its incidence will increase further as more men undergo PSA mass screening. Our study shows that the incidence of prostate cancer in RCP specimens from Japanese men is consistent with previous reports from the USA and Western Europe,[14–18] and similar to the reported incidences (22.5–34.6%) in Japanese autopsy cases.[9]

With regard to the age distribution of prostate cancer, Ashley showed that there is a linear relationship between the frequency of prostate cancer and age when plotted double logarithmically, and that its slope is 3.[25] In other words, the age-specific incidence of prostate cancer increases approximately with the third power of age.[25] Our present data are consistent with Ashley's classic paper (Fig. 5). Although Ashley considered that the development of prostate cancer requires three (epi)genetic events, based on the Armitage and Doll multistage carcinogenesis model,[26] our data should not be interpreted so simply; the number of (epi)genetic events required for prostate carcinogenesis cannot be determined solely on the basis of incidence data. However, we were able to confirm that prostate carcinogenesis is highly age dependent. Moreover, when we plotted the incidence of significant cancer on the same graph, the plot was linear with a slope of 4 (Fig. 5), indicating that progression to significant prostate cancer requires additional (epi)genetic events.

The PCPT revealed that a considerable proportion of men with low PSA values have prostate cancer.[6] Consequently, it has been suggested that the 'normal' PSA threshold should be discarded.[8] Moreover, there has been an argument that the significance of PSA as a tumor marker has been lost, and that PSA is better regarded as a marker of benign prostatic hyperplasia.[27] Thus, the significance of PSA in screening and prognostication

doi: 10.1111/j.1349-7006.2009.01267.x

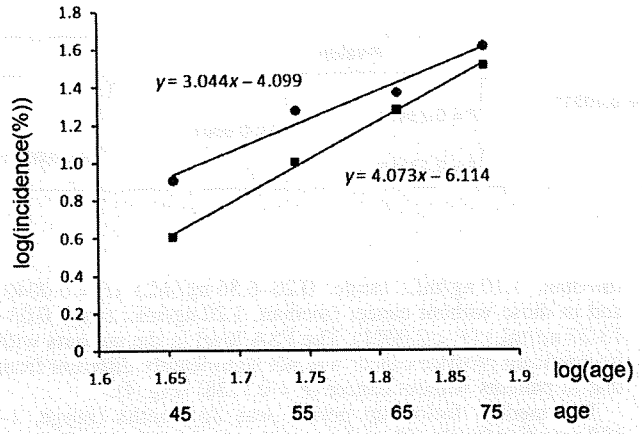

Fig. 5. Incidence of all (circles) and significant (squares) prostate cancers in every decade of patient age presented as a double logarithmic graph. Approximate lines are shown.

has recently been questioned. However, our present study indicates that increasing PSA levels are certainly associated with a higher incidence of all and significant prostate cancers. For example, the incidence of prostate cancer in patients with a PSA level ≥3 ng/mL (35/74, 47.3%) was significantly higher than in patients with a PSA level <3 ng/mL PSA (54/272, 19.9%) ($P < 0.0001$, χ^2-test). Thus, our data suggest that PSA would still be a useful screening tool for prostate cancer, at least in Japan where PSA screening is less prevalent than in Western countries.

In our study 73.5% of 'significant' cancers were small (less than 0.5 mL). Haas *et al.* reported that only 11% of cancers with a volume of less than 0.5 mL, which was estimated by computerized planimetry using an image analysis program, were detectable by 12-core biopsy in autopsy cases.[28] Therefore, most of the small 'significant' cancers in the present study would not have been detectable with current biopsy techniques. However, it is unlikely that all of these small 'significant' cancers need to be detected at such an early stage: McNeal reported that the probability of metastasis is correlated with cancer volume and grade.[11] In our present cohort of prostate cancers, we observed that most cancers with a Gleason score of ≥8 or with nodal metastasis had a volume of 0.5 mL or more (Fig. 1). Overlooking small 'significant' cancers would not compromise prognosis if patients were undergoing periodic PSA screening.

Eighteen of our patients had prostate cancers of 0.5 mL or more, which corresponds to a tumor approximately 1.0 cm in diameter. If PSA = 3.0 ng/mL were used as a threshold for recommending prostate biopsy, then 15 men with prostate cancers of 0.5 mL or more would have been included (sensitivity, 15/18 = 83.3%; specificity, 269/328 = 82.0%; positive predictive value, 15/74 = 20.3%). If PSA = 4.0 ng/mL were applied as a threshold, then an additional four men with prostate cancers of 0.5 mL or more would have been missed, resulting in lower sensitivity (11/18 = 61.1%). In addition, prostate biopsy does not always guarantee detection of all cancers with a volume of 0.5 mL or more. The threshold PSA level for prompting prostate biopsy needs to be determined carefully bearing these issues in mind.

Schröder *et al.* have reported that men with a PSA level of 3.0 ng/mL or less do not require immediate biopsy:[29] according to their analysis of data from the European Randomized Screening for Prostate Cancer Trial, which adopted 3.0 ng/mL PSA as a threshold to prompt biopsy, only six deaths from prostate cancer might have been prevented if all 15 773 eligible men with a PSA level of 3.0 ng/mL or less had undergone biopsy.

In summary, prostate cancer is a common finding in RCP specimens, with a significant proportion having the characteristics of clinically significant prostate cancer. Increasing patient age and PSA value are associated with a high incidence of all and significant prostate cancers, and PSA still appears to be a useful tool for prostate cancer screening

Disclosure Statement

The authors have no conflict of interest.

Abbreviations

ECE	extracapsular extension
PCPT	the Prostate Cancer Prevention Trial
PSA	prostate-specific antigen
RCP	radical cystoprostatectomy
SVI	seminal vesicle invasion

References

1 Jemal A, Siegel R, Ward E *et al.* Cancer statistics, 2008. *CA Cancer J Clin* 2008; **58**: 71–96.
2 Catalona WJ, Smith DS, Ratliff TL *et al.* Measurement of prostate-specific antigen in serum as a screening test for prostate cancer. *N Engl J Med* 1991; **324**: 1156–61.
3 Crawford ED, Thompson IM. Controversies regarding screening for prostate cancer. *BJU Int* 2007; **100**(Suppl 2): 5–7.
4 Catalona WJ, Smith DS, Ornstein DK. Prostate cancer detection in men with serum PSA concentrations of 2.6 to 4.0 ng/mL and benign prostate examination. Enhancement of specificity with free PSA measurements. *JAMA* 1997; **277**: 1452–5.
5 Punglia RS, D'Amico AV, Catalona WJ, Roehl KA, Kuntz KM. Effect of verification bias on screening for prostate cancer by measurement of prostate-specific antigen. *N Engl J Med* 2003; **349**: 335–42.
6 Thompson IM, Pauler DK, Goodman PJ *et al.* Prevalence of prostate cancer among men with a prostate-specific antigen level < or = 4.0 ng per milliliter. *N Engl J Med* 2004; **350**: 2239–46.
7 Welch HG, Schwartz LM, Woloshin S. Prostate-specific antigen levels in the United States: implications of various definitions for abnormal. *J Natl Cancer Inst* 2005; **97**: 1132–7.
8 Thompson IM, Ankerst DP, Etzioni R, Wang T. It's time to abandon an upper limit of normal for prostate specific antigen: assessing the risk of prostate cancer. *J Urol* 2008; **180**: 1219–22.
9 Yatani R, Shiraishi T, Nakakuki K *et al.* Trends in frequency of latent prostate carcinoma in Japan from 1965–79 to 1982–86. *J Natl Cancer Inst* 1988; **80**: 683–7.
10 Stamey TA, Freiha FS, McNeal JE, Redwine EA, Whittemore AS, Schmid HP. Localized prostate cancer. Relationship of tumor volume to clinical significance for treatment of prostate cancer. *Cancer* 1993; **71**(Suppl 3): 933–8.
11 McNeal JE. Prostatic microcarcinomas in relation to cancer origin and the evolution to clinical cancer. *Cancer* 1993; **71**(Suppl 3): 984–91.
12 Stein JP, Skinner DG. Radical cystectomy for invasive bladder cancer: long-term results of a standard procedure. *World J Urol* 2006; **24**: 296–304.
13 Kurokawa K, Ito K, Yamamoto T *et al.* Comparative study on the prevalence of clinically detectable prostate cancer in patients with and without bladder cancer. *Urology* 2004; **63**: 268–72.
14 Damiano R, Di Lorenzo G, Cantiello F *et al.* Clinicopathologic features of prostate adenocarcinoma incidentally discovered at the time of radical cystectomy: an evidence-based analysis. *Eur Urol* 2007; **52**: 648–57.
15 Hautmann SH, Conrad S, Henke RP *et al.* Detection rate of histologically insignificant prostate cancer with systematic sextant biopsies and fine needle aspiration cytology. *J Urol* 2000; **163**: 1734–8.
16 Ward JF, Bartsch G, Sebo TJ, Pinggera GM, Blute ML, Zincke H. Pathologic characterization of prostate cancers with a very low serum prostate specific antigen (0–2 ng/mL) incidental to cystoprostatectomy: is PSA a useful indicator of clinical significance? *Urol Oncol* 2004; **22**: 40–7.
17 Winkler MH, Livni N, Mannion EM, Hrouda D, Christmas T. Characteristics of incidental prostatic adenocarcinoma in contemporary radical cystoprostatectomy specimens. *BJU Int* 2007; **99**: 554–8.

18 Thomas C, Wiesner C, Melchior S, Gillitzer R, Schmidt F, Thüroff JW. Indications for preoperative prostate biopsy in patients undergoing radical cystoprostatectomy for bladder cancer. *J Urol* 2008; **180**: 1938–41.
19 Sobin LH, Fleming ID. *TNM Classification of Malignant Tumors*, 6th edn. Union Internationale Contre le Cancer and the American Joint Committee on Cancer, 2002.
20 Epstein JI, Allsbrook WC Jr, Amin MB, Egevad LL, ISUP Grading Committee. The International Society of Urological Pathology (ISUP) consensus conference on Gleason grading of prostatic carcinoma. *Am J Surg Pathol* 2005; **29**: 1228–42.
21 Noguchi M, Stamey TA, McNeal JE, Yemoto CE. Assessment of morphometric measurements of prostate carcinoma volume. *Cancer* 2000; **89**: 1056–64.
22 Marugame T, Mizuno S. Comparison of prostate cancer mortality in five countries: France, Italy, Japan, UK and USA from the WHO mortality database (1960–2000). *Jpn J Clin Oncol* 2005; **35**: 690–1.
23 Ito K, Yamamoto T, Takechi H, Suzuki K. Impact of exposure rate of PSA-screening on clinical stage of prostate cancer in Japan. *J Urol* 2006; **175**(Suppl): 477–8.
24 Sirovich BE, Schwartz LM, Woloshin S. Screening men for prostate and colorectal cancer in the United States: does practice reflect the evidence? *JAMA* 2003; **289**: 1414–20.
25 Ashley DJ. On the incidence of carcinoma of the prostate. *J Pathol Bacteriol* 1965; **90**: 217–24.
26 Armitage P, Doll R. The age distribution of cancer and a multi-stage theory of carcinogenesis. *Br J Cancer* 1954; **8**: 1–12.
27 Stamey TA, Caldwell M, McNeal JE, Nolley R, Hemenez M, Downs J. The prostate specific antigen era in the United States is over for prostate cancer: what happened in the last 20 years? *J Urol* 2004; **172**: 1297–301.
28 Haas GP, Delongchamps NB, Jones RF *et al*. Needle biopsies on autopsy prostates: sensitivity of cancer detection based on true prevalence. *J Natl Cancer Inst* 2007; **99**: 1484–9.
29 Schröder FH, Bangma CH, Roobol MJ. Is it necessary to detect all prostate cancers in men with serum PSA levels <3.0 ng/mL? A comparison of biopsy results of PCPT and outcome-related information from ERSPC. *Eur Urol* 2008; **53**: 901–8.

doi: 10.1111/j.1349-7006.2009.01267.x

Cancer Science
The official journal of the Japanese Cancer Association JCA

Quantitative proteomics using formalin-fixed paraffin-embedded tissues of oral squamous cell carcinoma

Ayako Negishi,[1,3] Mari Masuda,[1] Masaya Ono,[1] Kazufumi Honda,[1] Miki Shitashige,[1] Reiko Satow,[1] Tomohiro Sakuma,[6] Hideya Kuwabara,[6] Yukihiro Nakanishi,[2] Yae Kanai,[2] Ken Omura,[3,4,5] Setsuo Hirohashi[1] and Tesshi Yamada[1,7]

[1]Chemotherapy Division and [2]Pathology Division, National Cancer Center Research Institute, Chuo-ku, Tokyo; [3]Oral and Maxillofacial Surgery, [4]Department of Advanced Molecular Diagnosis and Maxillofacial Surgery, Hard Tissue Genome Research Center, and [5]Global Center of Excellence Program, International Research Center for Molecular Science in Tooth and Bone Diseases, Tokyo Medical and Dental University, Bunkyo-ku, Tokyo; Department of Surgery, [6]BioBusiness Group, Mitsui Knowledge Industry, Minato-ku, Tokyo, Japan

(Received April 2, 2009/Revised May 12, 2009/Accepted May 13, 2009/Online publication June 11, 2009)

Clinical proteomics using a large archive of formalin-fixed paraffin-embedded (FFPE) tissue blocks has long been a challenge. Recently, a method for extracting proteins from FFPE tissue in the form of tryptic peptides was developed. Here we report the application of a highly sensitive mass spectrometry (MS)-based quantitative proteome method to a small amount of samples obtained by laser microdissection from FFPE tissues. Cancerous and adjacent normal epithelia were microdissected from FFPE tissue blocks of 10 squamous cell carcinomas of the tongue. Proteins were extracted in the form of tryptic peptides and analyzed by 2-dimensional image-converted analysis of liquid chromatography and mass spectrometry (2DICAL), a label-free quantitative proteomics method developed in our laboratory. From a total of 25 018 peaks we selected 72 mass peaks whose expression differed significantly between cancer and normal tissues ($P < 0.001$, paired t-test). The expression of transglutaminase 3 (TGM3) was significantly down-regulated in cancer and correlated with loss of histological differentiation. Hypermethylation of *TGM3* gene CpG islands was observed in 12 oral squamous cell carcinoma (OSCC) cell lines with reduced TGM3 expression. These results suggest that epigenetic silencing of TGM3 plays certain roles in the process of oral carcinogenesis. The method for quantitative proteomic analysis of FFPE tissue described here offers new opportunities to identify disease-specific biomarkers and therapeutic targets using widely available archival samples with corresponding detailed pathological and clinical records. (*Cancer Sci* 2009; 100: 1605–1611)

Squamous cell carcinoma is the major histological type of oral cancer and develops in various anatomical locations within the oral cavity, including the tongue, bucca, oropharynx, gingiva, palate, lip, and floor of the mouth. Despite recent improvements in surgical techniques and chemo/radiotherapy,[1] the overall 5-year survival rate for patients with oral squamous cell carcinoma (OSCC) is still unsatisfactory.[2] OSCC has a propensity for rapid local invasion and spread[3] and is considered to be one of the most aggressive forms of squamous cell carcinoma of the head and neck region. Furthermore, the incidence of OSCC has been increasing among the young and middle-aged.[4–6] Therefore, there is an urgent need to develop new diagnostic and therapeutic modalities to improve the outcome of OSCC. Although there is considerable epidemiological evidence for a significant association of alcohol consumption, tobacco smoking, chronic mechanical stimulation, and betel quid chewing with the incidence of OSCC, the molecular mechanisms responsible for OSCC have not been fully elucidated. Overall gene expression in OSCC has been studied extensively over the past decade using microarray techniques. However, gene expression is not always correlated with the expression levels of the corresponding proteins.[7] Although it is anticipated that protein expression reflects more directly the biological and pathological status of diseases, aberrations of protein expression during the course of oral carcinogenesis are largely unknown.

Although the use of fresh material is desirable for any analytical technology, human tissue samples are not always available in sufficient quantity. Formalin-fixed paraffin-embedded (FFPE) tissue blocks are routinely preserved and stored after pathological diagnosis, and such archived material may provide an ample alternative resource for research purposes. However, FFPE specimens have usually not been used for proteomic analyses, as formaldehyde-induced intermolecular and intramolecular cross-linking hinders the solubility of proteins and complicates the extraction of intact proteins from the samples.[8] Recently, a method of extracting proteins from FFPE tissues in the form of tryptic peptides was developed, and the methodology is compatible with a variety of subsequent mass spectrometry (MS)-based proteome applications.[9,10]

We previously developed a MS-based quantitative proteome platform named 2DICAL (2-dimensional image converted analysis of liquid chromatography and mass spectrometry)[11] for quantitative comparison of large peptide datasets generated by nano-flow liquid chromatography and mass spectrometry (LC-MS). Owing to its simple procedure, 2DICAL is highly sensitive and reproducible: 60 000–160 000 peptides can be readily detected in a 1-h LC run and accurately quantified without isotope labeling. In the present study we used 2DICAL for quantitative analysis of small samples of protein obtained from FFPE tissues by laser microdissection and searched for proteins that were differentially expressed between normal and cancerous epithelia of the oral cavity. Here we report the identification of transglutaminase 3 (*TGM3*) as an epigenetically silenced gene in OSCC cell lines.

Materials and Methods

Clinical samples and cell lines. FFPE tissues ($n = 63$) were collected from OSCC patients who underwent surgery at two medical institutions: the National Cancer Center Hospital (NCCH; Tokyo, Japan) between April 1997 and March 2006, and the Tokyo Medical and Dental University Hospital (TMDUH; Tokyo, Japan) between January 2001 and December 2006. All the patients were preoperatively diagnosed as having squamous cell carcinoma of the tongue. Surgically removed tongue tissues were routinely processed for pathological examination, fixed in formalin, embedded in paraffin,

[7]To whom correspondence should be addressed. E-mail: tyamada@ncc.go.jp

doi: 10.1111/j.1349-7006.2009.01227.x

and stored at room temperature. Pathological examination confirmed the histology of invasive squamous cell carcinoma. None of the patients had received preoperative radiation, chemotherapy, or immunotherapy. The cases were followed up for at least 3 years after surgery. Fresh oral mucosa was donated by a volunteer who had no history of malignancy. The protocol of the study was reviewed and approved by the ethics committee boards of the NCC and TMDU.

Twelve OSCC cell lines (Ca9-22, Ho-1-N-1, Ho-1-u-1, HSC-2, HSC-3, HSC-4, HSC-6, KON, KSOC-2, KSOC-3, SAS, SKN-3) were obtained from the Japan Health Science Foundation (Osaka, Japan) and cultured in Dulbecco's modified Eagle medium supplemented with 10% fetal bovine serum.

A plasmid expressing TGM3 (namely pcDNA3.1/TGM3) was constructed by cloning the full-length coding sequence of TGM3 cDNA into the pcDNA3.1 vector (Invitrogen, Carlsbad, CA, USA). pcDNA3.1/TGM3 or the control empty vector (pcDNA3.1) was transfected into cells using the Lipofectamine LTX reagent (Invitrogen).

Laser microdissection and peptide extraction. Paired tumor and adjacent normal epithelial cells were collected from the same FFPE tissues of the NCCH cases ($n = 10$). To recover cell populations of interest without contamination, we used laser microdissection. Ten-micrometer-thick FFPE sections were placed on DIRECTOR Laser Microdissection Slides (Expression Pathology, Gaithersburg, MD, USA), deparaffinized, and stained with hematoxylin–eosin (HE). Parts of the sections 3 mm^2 in area (corresponding to approximately 10 000 cells) were then microdissected using a LMD6000 (Leica Microsystems, Wetzlar, Germany). Proteins were extracted in the form of tryptic peptides utilizing a Liquid Tissue MS Protein Partitioning Kit (Expression Pathology) in accordance with the manufacturer's protocol. In brief, the microdissected tissues were suspended in Liquid Tissue buffer, incubated at 95°C for 90 min, and then cooled on ice for 3 min. Trypsin (15–18 units) was added, and the samples were incubated at 37°C overnight. Dithiothreitol was added to a final concentration of 10 mM, and the samples were heated for 5 min at 95°C. The extracted peptide samples were stored at –80°C until analysis.

Liquid chromatography and mass spectrometry (LC-MS). Twenty tissue samples (10 paired cancer and normal tissues) were blinded, randomized, and measured in triplicate with a linear gradient of 0–80% acetonitrile in 0.1% formic acid at a speed of 200 nL/min for 60 min using a nano-flow high-performance liquid chromatograph (HPLC) (NanoFrontier nLC; Hitachi High-technologies, Tokyo, Japan) connected to an electrospray ionization quadrupole time-of-flight (ESI-Q-TOF) mass spectrometer (NanoFrontier LD, Hitachi High-technologies) every second in the 400–1600 mass-to-charge ratio (m/z) range. MS peaks were detected, normalized, and quantified using in-house 2DICAL software, as described previously.[11] A serial identification (ID) number was applied to each detected MS peak, from ID1 to ID25018.

Protein identification by tandem mass spectrometry (MS/MS). MS/MS spectra were acquired from preparative LC. LC-MS data were aligned with a tolerance of ±0.5 m/z and a retention time (RT) of ±0.4 min, and targeted MS/MS was performed. Peak lists were generated using the MassNavigator software package (Version 1.2; Mitsui Knowledge Industry, Tokyo, Japan) and searched against the NCBInr database (NCBInr_20070419.fast) using the Mascot software package (Version 2.2.1; Matrix Sciences, London, UK). Initial peptide tolerances in MS and MS/MS modes were ±0.05 Da and ±0.1 Da, respectively. Trypsin was designated as the enzyme, and up to one missed cleavage was allowed. The score threshold to achieve $P < 0.05$ is set by the Mascot algorithm, based on the size of the database used in the search.

Immunohistochemistry (IHC). FFPE sections of NCCH ($n = 10$) and TMDUH ($n = 53$) cases were used for IHC. Immunoperoxidase staining was performed using the avidin–biotin–proxidase complex method as described previously.[12,13] Mouse monoclonal anti-TGM3 (1:150; Abnova, Taipei, Taiwan), anti-cytokeratin 4 (CK4) (1:200; Chemicon, Rosemont, IL, USA), anti-cytokeratin 13 (CK13) (1:200; Abcam, Cambridge, UK), and anti-annexin A1 (ANXA1) (1:200; BD Bioscience, Pharmingen, NJ, USA) antibodies and relevant secondary biotin-conjugated antibodies (1:200; Vector Laboratories, Peterborough, UK) were used. Two investigators (K.H., A.N.) blinded to the clinical data reviewed the stained sections. Normal tongue epithelium in the same section served as an internal positive control. Cases in which 10% or more of the tumor cells were positively stained with anti-TGM3 antibody were considered to be TGM3-positive, while cases in which less than 10% of the tumor cells were TGM3-positive were considered to be TGM3-negative. If considerable tumor heterogeneity was present, staining was evaluated in the predominantly differentiated area of the tumor.

Immunoblot analysis. Cells were washed with phosphate-buffered saline and lyzed in cell lysis buffer (50 mM Tris-HCl pH 7.5, 1% Triton-X100, 150 mM NaCl, 20 mM EDTA). The cell lysates were analyzed by immunoblotting, as described previously,[13] using anti-TGM3 (Abcam), CK14 (Thermo Scientific, Waltham, MA, USA), anti-involucrin (Thermo Scientific), and anti-β-actin (Sigma, St Louis, MO, USA) antibodies.

Cytosine methylation analysis. The detection of CpG islands and design of PCR primers for amplification were performed by Methyl Primer Express Software v1.0 (Applied Biosystems, Foster City, CA, USA). Genomic DNA was extracted using DNeasy Blood and Tissue kits (Qiagen, Valencia, CA, USA). Bisulfite conversion was carried out using 2 μg of genomic DNA and the reagents provided in EpiTect Bisulfite Kit (Qiagen). The converted DNA was subjected to PCR using primer sets (5′-GTTTAAATAAAGG TATTTGGTTTAGAG-3′ and 5′-CTTACCCATACTACTCATACC CAC-3′). The PCR products were visualized by 3% agarose gel electrophoresis and subcloned into the TA vector using a TOPO TA Cloning Kit (Invitrogen). Eight colonies were sequenced using an ABI 3130 (Applied Biosystems).

Real-time reverse-transcription PCR. Cells were treated with 0, 2, or 5 μM 5′-aza-2′-deoxycytidine (5Aza-dC) for 5 days. Total RNA was prepared with an RNeasy Mini Kit (Qiagen). DNase-I-treated RNA was random-primed and reverse-transcribed using a High Capacity RNA-to-cDNA Kit (Applied Biosystems). The TaqMan universal PCR master mix and predesigned TaqMan Gene Expression probe and primer sets were purchased from Applied Biosystems. Amplification data measured as an increase in reporter fluorescence were collected using a PRISM 7000 Sequence Detection system (Applied Biosystems). The level of messenger RNA (mRNA) expression relative to the internal control (β-actin) was calculated by the comparative threshold cycle (C_T) method.[14]

Statistical analysis. Differences between subgroups were tested with paired *t*-test. The clinicopathological variables pertaining to the corresponding patients were analyzed for statistical significance by Fisher's exact test. Statistical analyses were performed using an open-source statistical language R (version 2.7.0) with the optional module design package.

Results

Identification of proteins differentially expressed in tongue cancer. Parts corresponding to an area of 3 mm^2 (approximately 10 000 cells) were microdissected from cancerous and adjacent normal epithelia that lacked significant contamination with infiltrating inflammatory cells, stromal cells, muscular components, vascular components, and necrotic cells (Fig. 1a). Then, 20 paired protein samples were prepared from 10 tongue squamous cell carcinoma (TSCC) cases and analyzed for differential protein expression profiles using the 2DICAL proteome platform. A total of 25 018 MS peaks per sample were readily detected and quantified. Linear regression analysis demonstrated excellent linearity with a mean

doi: 10.1111/j.1349-7006.2009.01227.x

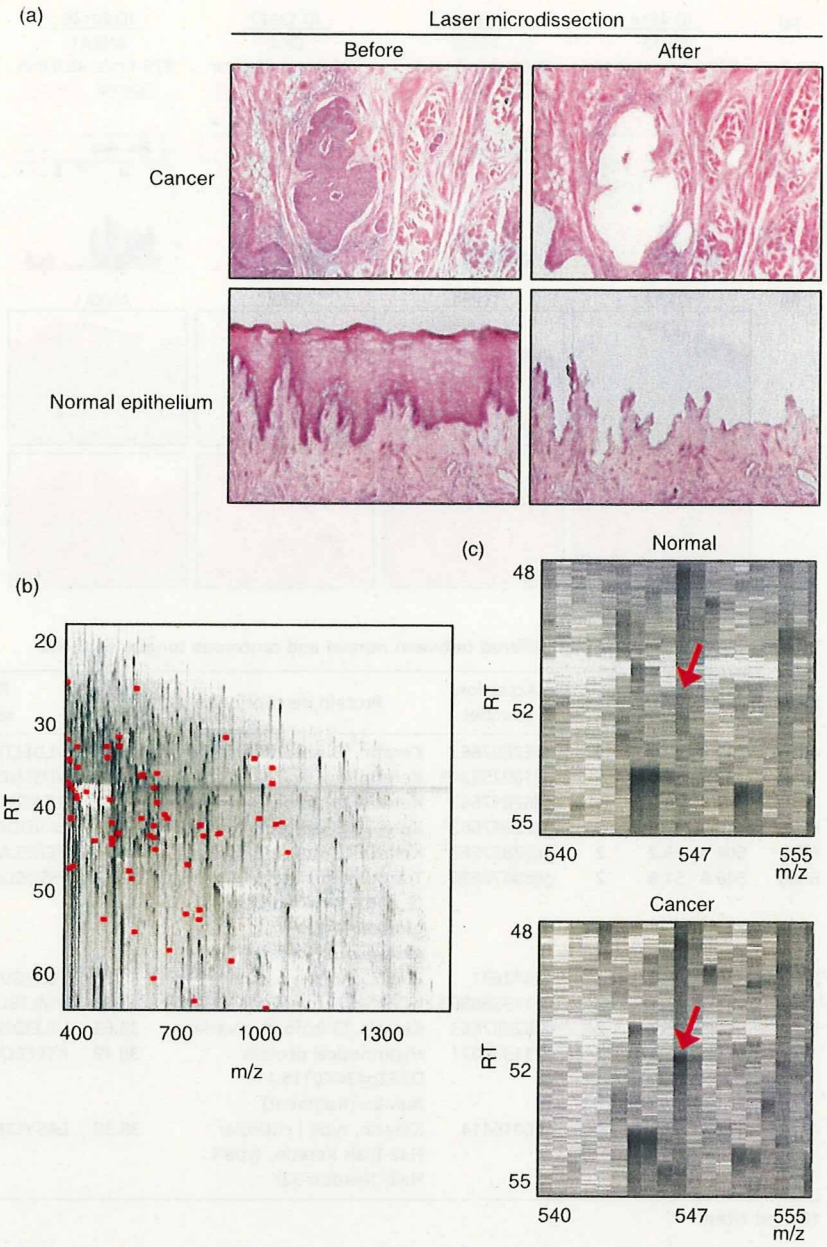

Fig. 1. Identification of proteins differentially expressed in tongue squamous cell carcinoma (TSCC) by 2-dimensional image-converted analysis of liquid chromatography and mass spectrometry (2DICAL). (a) Selective removal of cancerous and normal tongue epithelia from formalin-fixed paraffin-embedded (FFPE) tissues. The microscopic appearances (HE staining) of cancer (top; magnification, ×100) and normal tongue (bottom; magnification, ×40) tissues before (left) and after (right) laser microdissection are shown. (b) Two-dimensional display of all (>25 000) MS peaks of a representative sample with the m/z-values (400–1600 m/z) along the horizontal (*x*) axis and retention time (RT) (20.0–63.0 min) along the vertical (*y*) axis. The 72 MS peaks whose average intensity of triplicates differed significantly between cancer and normal epithelia ($P < 0.001$ [paired *t*-test]) are highlighted in red. (c) Close-up view of a representative MS peak whose intensity differed significantly between normal (top) and cancerous (bottom) epithelia (indicated by red arrows).

correlation coefficient (CC) of 0.9954 (0.9794–0.9989) for the entire 25 018 MS peaks between triplicates (Suppl Fig. S1), confirming the high reproducibility of 2DICAL. The MS peaks detected in a representative run are displayed with m/z along the *x* axis and RT along the *y* axis (Fig. 1b).

Among the total of 25 018 MS peaks, we found 72 whose average intensity of triplicates differed significantly between cancer and normal epithelia as a relatively strict criterion ($P < 0.001$ [paired *t*-test] and average peak intensity >100 [arbitrary unit] for either cancer or control samples) (Fig. 1b, indicated in red; Fig. 1c, indicated by arrows). The intensity of 10 peaks was increased in cancer and that of the remaining 62 peaks was decreased (data not shown). We further selected 12 peaks whose intensity was decreased in cancer by visually inspecting the aligned raw MS spectra (Fig. 2a, top, highlighted in green boxes) and the mean peak intensity (Fig. 2a, bottom) across the 20 samples. A database search using the NCBInr (NCBInr_20070419.fast) for the MS/MS spectra of the 12 peaks identified the amino acid sequences of seven proteins with significant confidence ($P < 0.05$) (Table 1 and Suppl Figs S2–5).

The decreased expression of four proteins, for which antibodies were available, was validated by IHC in 10 TSCC surgical specimens (NCCH) (Fig. 2b). Intense positive immunoreactivity for TGM3, CK13, CK4, and ANXA1 was detected in normal tongue epithelia. Cancerous lesions evidently demonstrated down-regulation of these proteins. ANXA1 staining was observed in all the layers of normal epithelia, whereas only keratinized, but living, cancer cells showed moderate staining for ANXA1 (Fig. 2b). Among these proteins differentially expressed in TSCC, we decided to focus on gaining further insight into the characteristics of TGM3, whose roles in oral carcinogenesis have remained unclear.

Clinicopathological significance of TGM3. To assess the clinical significance of TGM3, its expression was evaluated by IHC in a larger cohort consisting of 53 TSCC cases (TMDUH) (Suppl

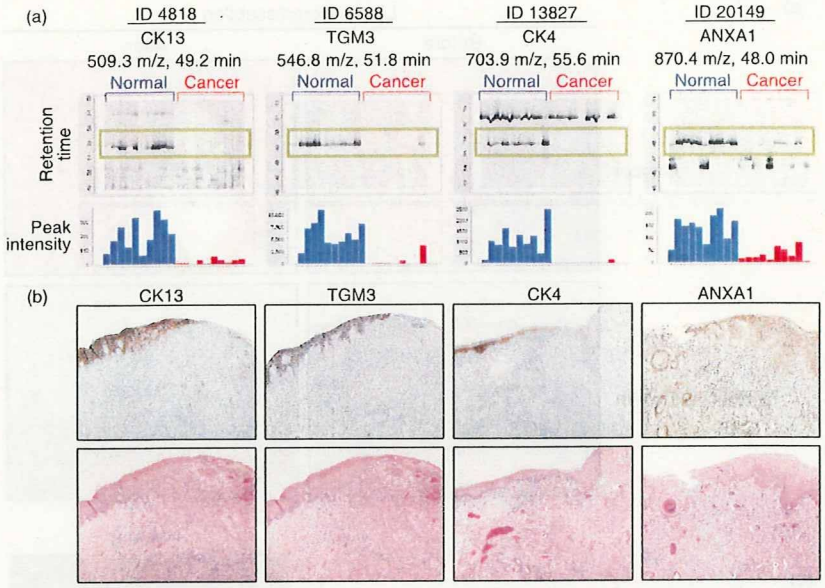

Fig. 2. Identification and validation of differentially expressed proteins. (a) Gel-like views of MS peaks with retention time (RT) along the vertical axes (top) and distribution of the mean peak intensity of triplicates (bottom) across 20 samples (60 liquid chromatography and mass spectrometry [LC-MS] runs). Cancer tissues (red) exhibit reduced expression of the four indicated proteins compared with normal epithelia (blue). (b) Immunoperoxidase staining of CK13, TGM3, CK4, and ANXA1 proteins in tongue squamous cell carcinoma (TSCC) (top) (magnification, ×40). Images of corresponding HE-stained serial sections are shown at the bottom.

Table 1. List of peptides that differed between normal and cancerous tongue epithelia

ID	M/Z	RT	Charge	Accession number	Protein description	Mascot score	Peptide sequence	Normal (mean ± SD)	Cancer (mean ± SD)	*P*-values*
4818	509.3	49.2	2	gi|62897663	Keratin 13 isoform a variant	73.89	VLDELTLSK	6088 ± 2506	491 ± 149	2.56E-04
13 827	703.9	55.6	2	gi|109255249	Keratin 4	59.37	VDSLNDEINFLK	1078 ± 633	23 ± 4	8.76E-04
7777	572.9	44.2	2	gi|62897663	Keratin 13 isoform a variant	54.31	ILTATIENNR	4338 ± 1645	233 ± 82	1.09E-04
673	418.2	47.6	2	gi|62897663	Keratin 13 isoform a variant	53.6	LAVDDFR	9241 ± 3859	848 ± 474	2.51E-04
4572	504.3	46.2	2	gi|62897663	Keratin 13 isoform a variant	47.73	YENELALR	5147 ± 2130	303 ± 95	1.77E-04
6588	546.8	51.8	2	gi|80478896	Transglutaminase 3 (E polypeptide, protein-glutamine-gamma-glutamyltransferase)	42.36	FSSQELILR	209 ± 103	21 ± 15	6.36E-04
20 149	870.4	48.0	2	gi|442631	Chain, annexin I	41.86	SEDFGVNEDLADSDAR	141 ± 51	32 ± 19	5.41E-04
1203	431.3	43.5	2	gi|119568898	hCG1643722, isoform CRA_b	41.57	VMLTELR	9947 ± 4751	561 ± 163	4.78E-04
5504	521.8	48.7	2	gi|62897663	Keratin 13 isoform a variant	38.65	VILEIDNAR	9570 ± 2752	890 ± 302	3.04E-05
12 366	673.4	55.1	2	gi|11360071	Hypothetical protein DKFZp434K0115.1 – human (fragment)	38.49	KTLEEQISEIR	1757 ± 615	73 ± 9	3.40E-05
434	412.3	42.9	2	gi|6016414	Keratin, type I cuticular Ha2 (hair keratin, type I Ha2) (keratin-32)	38.38	LASYLTR	5312 ± 2562	359 ± 91	5.88E-04

†Paired *t*-test.

Fig. S6). In normal tongue mucosa, TGM3 immunoreactivity was confined to the spinous and parakeratinized layers of epithelial cells (Suppl Fig. S6a). Strong nuclear staining for TGM3 was seen in the spinous layer, whereas cytoplasmic staining was detected in the parakeratinized layers. Only 12 out of 53 TSCC cases were positive for TGM3 expression (Table 2). Most cancer cells exhibited sparse immunoreactivity for TGM3 (Suppl Fig. S6c–e) and, when detected, the staining tended to be localized in the differentiated and keratinized area of TSCC (Suppl Fig. S6b). Statistical analysis of the correlation between TGM3 expression and clinicopathologic characteristics demonstrated that TGM3 expression was inversely correlated with loss of histological differentiation ($P < 0.05$, Fisher's exact test), but not with other clinicopathological variables including age, sex, and TNM classification (Table 2).

Lack of TGM3 expression in OSCC cells and its restoration by 5Aza-dC. We next examined TGM3 protein expression in 12 OSCC cell lines by immunoblot analysis. None of these cell lines expressed TGM3 protein. Some of the OSCC cell lines expressed differentiation-associated markers of squamous epithelia, such as CK14 for the proliferative basal layer and involucrin for the upper differentiating layer (Fig. 3a). Real-time PCR analysis to quantify the *TGM3* mRNA expression of these cells gave results consistent with those obtained by immunoblot analysis (data not shown). In an attempt to investigate the molecular mechanism of the gene silencing of *TGM3* in OSCC cells, we grew Ca9-22 cells lacking TGM3 expression in the presence of a methyltransferase inhibitor, 5Aza-dC, for 5 days. Real-time PCR analysis revealed a dose-dependent increase of *TGM3* mRNA expression, and 5-μM 5Aza-dC increased the expression of *TGM3* up to ~60 fold over untreated cells (Fig. 3b). Similar results were obtained in other OSCC cell lines treated with 5Aza-dC (data not shown). Since histone deacetylation, which is catalyzed by the histone deacetylase family, is known to mediate transcriptional repression, we treated Ca9-22 cells with a histone deacetylase inhibitor trichostatin A,

doi: 10.1111/j.1349-7006.2009.01227.x